

STABILITY STUDY OF A NONLINEAR
SAMPLED-DATA CONTROL
SYSTEM

By

WILLIAM STAHLEY

Bachelor of Science
Oklahoma State University
Stillwater, Oklahoma
1957

Master of Science
Oklahoma State University
Stillwater, Oklahoma
1959

Submitted to the Faculty of the Graduate School
of the Oklahoma State University
in partial fulfillment of
the requirements for
the degree of
DOCTOR OF PHILOSOPHY
May, 1964

JAN 8 1955

STABILITY STUDY OF A NONLINEAR
SAMPLED-DATA CONTROL
SYSTEM

Thesis Approved:

James D. ...

Thesis Adviser
Paul A. McCollum

W. J. Bentley

E. J. Waller

Robert Morrison

J. H. Boyce

Dean of the Graduate School

570378

ACKNOWLEDGMENTS

The author wishes to acknowledge the opportunity awarded him by the School of Electrical Engineering in providing a graduate assistantship which made it financially possible to complete the graduate work at Oklahoma State University.

He also wishes to thank Dr. Harold T. Fristoe for serving as Chairman of the Advisory Committee and for his helpful guidance throughout the entire Ph.D. program. In addition, the author is greatly indebted to the other members of the Committee: Professors Wilson J. Bentley, Edwin J. Waller, Paul A. McCollum, and Dr. Robert D. Morrison, who contributed much to the success of the program.

Finally, the author would like to thank his wife, Ednamae, for her continued encouragement throughout the graduate program, and for her assistance in the preparation of this thesis.

TABLE OF CONTENTS

Chapter	Page
I. INTRODUCTION	1
II. SYSTEM ANALYSIS	4
III. ANALYTICAL STUDY	14
Frequency Phase Plot for $HG^*(j\omega)$	15
Approximation for the Nonlinear Element	22
Improved Approximation for $N(\alpha) HG^*(j\omega)$	27
Example of the Method	28
IV. EXPERIMENTAL STUDY	44
System Used for the Study	45
Method Used to Obtain Results	47
Results Obtained From the Experimental Analysis	49
V. SUMMARY AND ANALYSIS OF RESULTS	52
Analysis of the Results	56
VI. CONCLUSIONS	64
BIBLIOGRAPHY	68

LIST OF TABLES

Table	Page
I. Relative Magnitudes of the Fundamental and Third Harmonics for Two Degrees of Saturation	36
II. Percentage Third Harmonic for Two Degrees of Saturation	36
III. Calculated Open-Loop Response of the Nonlinear Sampled-Data Control System	40
IV. Experimental Results	50

LIST OF FIGURES

Figure	Page
1. Typical Nonlinear Sampled-Data Control System	6
2. Nyquist Diagram	10
3. Stable and Unstable Plots on a Nyquist Diagram	11
4. M-Circles and Frequency Phase Plot	12
5. The Sampler and Waveforms of Input and Output .	17
6. Periodicity Strips of $X^*(s)$ in the s-Plane . .	17
7. Frequency Spectra of the Original and the Sampled Signal	18
8. Frequency Spectrum of Sampler Output When Sampling Frequency is Less Than Twice the Highest Input Signal.	19
9. Construction of the Frequency Phase Plot for $HG^*(j\omega)$	23
10. Input-Output Characteristics of Nonlinear Elements	24
11. Output of Saturation Type Nonlinearity With Sinusoidal Input	29
12. Method for Constructing the Nonlinear Sampled-Data Frequency Phase Loci	32
13. Magnitude of Harmonics for Saturated Sine Wave	34
14. Two Degrees of Saturation	35
15. Nonlinear Sampled-Data Control System	37
16. Waveforms at the Input and Output of a Zero-Order Hold Circuit	38

Figure	Page
17. Frequency Characteristics of the Nonlinear Sampled-Data Control System	41
18. Analog Computer Circuit for Forward Transfer Function	45
19. Circuit for Generating Nonlinearity Along With Input and Output Waveforms	47
20. Analog Computer Schematic of the Nonlinear Sampled-Data Control System	48
21. Output Waveforms From Sampler and Hold Circuit.	59
22. Calculated and Experimental Response of the Linear Sampled-Data Control System ($\alpha = 90^\circ$) .	60
23. Calculated and Experimental Response of the Nonlinear Sampled-Data Control System ($\alpha = 51^\circ$)	62
24. Calculated and Experimental Response of the Nonlinear Sampled-Data Control System ($\alpha = 23^\circ$)	63

CHAPTER I

INTRODUCTION

During the past decade there has been a number of books and many articles appearing in technical journals and written on the subject of the design and analysis of digital or sampled-data control systems. The great interest in this area of control engineering was brought about when digital equipment was used to replace much of the analog equipment in control systems. The digital equipment can handle only discrete information; therefore, the continuous data from the other sections of the system must be sampled in order to be of use.

Although a great deal has been written about the analysis of linear sampled-data control systems, very little has been said concerning nonlinear systems. There are two reasons why the study of nonlinear sampled-data control systems is important: first, practically all components used in a control system are nonlinear, unless they are restricted to operate over a limited range; and, second, in recent years control engineers have deliberately introduced nonlinear elements in the control system to improve the performance of the over-all system. Therefore, in view of the importance and lack of information in

this area, this thesis will be a presentation of a method of analysis of nonlinear sampled-data control systems.

The work to date in this field has been presented primarily in three papers. The first was written by Mullin in July, 1959.¹ In his paper he examined the stability of saturating sampled-data systems by investigating the roots of its characteristic equation. The next paper to appear was written by Tou and Kinnen in January, 1960.² They presented a method for obtaining the transient response of nonlinear sampled-data systems. The third paper was written by Aseltine and Nesbit in August, 1960, in which they described a phase plane method of analysis for nonlinear sampled-data control systems.³ There have been other authors who mentioned nonlinearities in their discussion of linear sampled-data systems; however, their study was very limited.

In view of the fact that very little has been reported on the analysis of nonlinear sampled-data control systems using the real frequency domain, this study will be an

¹F. J. Mullin, "Stability of Saturating Sampled-Data Systems," American Institute of Electrical Engineers-Part I Communications and Electronics (July, 1959), p. 270.

²Tou and Kinnen, "Analysis of Nonlinear Sampled-Data Control Systems," American Institute of Electrical Engineers Transactions-Part II Application and Industry (January, 1960), pp. 386-394.

³J. A. Aseltine and R. A. Nesbit, "The Incremental Phase Plane for Nonlinear Sampled-Data Systems," Transactions of Institute of Radio Engineers on Automatic Control (August, 1960), pp. 159-165.

analysis in that domain. The graphical tool to be used in this analysis will be the Nyquist diagrams. These diagrams are polar plots of the magnitude and phase of the systems open-loop transfer function which will be referred to hereafter as frequency phase plot. Once the frequency phase plot has been obtained, the system's degree of stability may be found by employing the conventional methods of analysis for linear continuous-data systems. Therefore, this thesis will be limited to the problem of obtaining a frequency phase plot for nonlinear sampled-data control systems.

The type of nonlinearities to be considered here are ones in which the mode of operation of the system changes rapidly compared to its response time. Saturation, dead zone, and backlash or hysteresis are examples of this type.

CHAPTER II

SYSTEM ANALYSIS

Much of the control engineer's time is taken up with studies of system stability. He must determine if the output of a system is finite when a bounded signal is applied to the input. There are several techniques which he may use for examining this problem. In some cases one technique may yield better results than another, and many times several will be employed before the desired results are obtained. One technique which has proved to be very useful in the design of linear and nonlinear continuous-data systems, and also linear sampled-data control systems is the Nyquist diagram. If this technique could be extended to include nonlinear sampled-data control systems, the control engineer would have added to his repertoire a very useful tool. This study will be an investigation into the problem of making that extension.

The basic background information for this thesis is presented in this chapter. This includes a thorough discussion of the system under study, the derivations of the transfer function of the system, the stability considerations, and the Nyquist diagram for stability study of nonlinear sampled-data control systems. A considerable amount

of space is devoted to this background information in order to illustrate that Nyquist diagrams can be used to determine the relative stability of nonlinear sampled-data control system as well as to linear continuous-data system.

The block diagram of a typical nonlinear sampled-data control system is shown in Figure 1. The blocks designated by $G(s)$ and $H(s)$ are the linear transfer functions of the forward and feedback paths, respectively. $N(\alpha)$ is the nonlinear element of the system which may be either the sum of all the incidental nonlinearities of the system, or a nonlinear element which has been intentionally introduced to improve the performance of the system. The names and designations of the signals are: input, $R(s)$; output, $C(s)$; actuating, $E(s)$; sampled actuating, $E^*(s)$; and feedback, $B(s)$. The signal from the output of the nonlinear element is designated by y , and will be discussed later in this study. The sampler is designated by S and is shown here in the actuating signal line; however, it could be, and often is, located in other signal lines. When the sampler is placed in another line the analysis of the system is carried out in the same manner as will be given here; however, the results are likely to be different. There are many cases also where more than one sampler is used in the system, and again only the results will change and not the method given here.

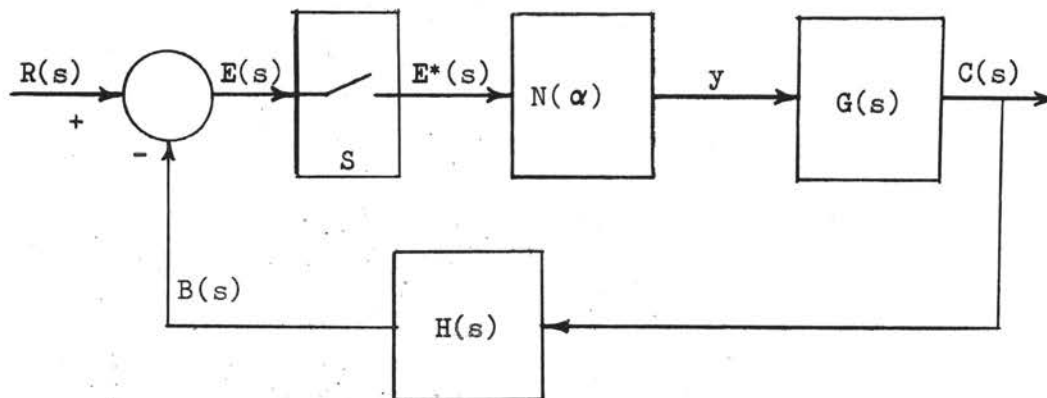


Figure 1. Typical Nonlinear Sampled-Data Control System

The transfer function of a system is defined as the ratio of the output transform of the system to its input transform. The transfer function for the system shown in Figure 1 can be derived by referring to the figure and observing that

$$C(s) = E^*(s) N(\alpha) G(s), \quad (1)$$

$$B(s) = C(s) H(s), \quad (2)$$

and

$$E(s) = R(s) - B(s). \quad (3)$$

Substituting $C(s)$, from Equation 1, into Equation 2 and substituting this result for $B(s)$ into Equation 3 will yield

$$E(s) = R(s) - E^*(s) N(\alpha) G(s) H(s). \quad (4)$$

The sampler is a linear device, which means that the law of superposition is valid; therefore, Equation 3 may be written

$$E^*(s) = R^*(s) - B^*(s). \quad (5)$$

The symbol * indicates that the signal has been sampled at a fixed rate. Equation 4 may now be written

$$E^*(s) = R^*(s) - E^*(s) N(\alpha) HG^*(s). \quad (6)$$

The term $HG^*(s)$ indicates that $H(s)$ and $G(s)$ are multiplied before sampling, which is not the same as sampling the output of $G(s)$ prior to applying the signal to $H(s)$. In the latter case the operation would be represented by $G^*(s) H^*(s)$. Solving Equation 6 for $E^*(s)$ and substituting that back into Equation 1 yields

$$C(s) = \frac{R^*(s) N(\alpha) G(s)}{1 + N(\alpha) HG^*(s)}, \quad (7)$$

the output of the system. Dividing each side of Equation 7 by $R^*(s)$, the sampled input, yields

$$\frac{C(s)}{R^*(s)} = \frac{N(\alpha) G(s)}{1 + N(\alpha) HG^*(s)}. \quad (8)$$

Equation 8 is the transfer function of the nonlinear sampled-data control system shown in Figure 1. This equation differs slightly from the definition of a transfer function given above, in that this is a ratio of the output transform to the sampled input transform, instead of

the ratio of the output transform to the input transform. Additional information concerning sampled-data transfer functions has been given by Tou.¹

In a stability study, the fact that the input signal has been sampled will have no effect, because the definition of stability states that the output of the system must be finite when a bounded signal is applied to the input. The signal from the sampler is only the function value of the signal prior to sampling; therefore, the sampled signal will be bounded if the signal, prior to sampling, is bounded. Thus, the stability of the system may be determined the same way as linear continuous-data control systems: by examining the poles of Equation 8, or the zeros of

$$1 + N(\alpha) HG^*(s) = 0. \quad (9)$$

Equation 9 is the denominator of Equation 8 set equal to zero. All the roots of this equation must be located in the left half of the s-plane in order to have a stable system. An outline of the proof of this has been given by Tou for continuous-data and sampled-data control systems.^{2, 3}

¹J. T. Tou, Digital and Sampled-Data Control Systems (New York, 1959), pp. 115-117.

²Ibid, pp. 20-23.

³Ibid, p. 125.

The method which is used for the detection of roots of Equation 9 not in the left half of the s -plane is the Nyquist diagram. This diagram is essentially a mapping of the entire right half of the s -plane into the HG-plane. The HG-plane is an open loop transfer function plane on which a frequency phase plot of $N(\alpha) HG^*(s)$, with s replaced with $j\omega$ and ω varied from zero to infinity, is plotted. This plot on the HG-plane is called the Nyquist diagram. Nyquist did the original work to show that roots of Equation 9, which lie in the right half of the s -plane, will cause the frequency phase plot of $N(\alpha) HG^*(j\omega)$ to encircle the critical point $(-1 + j0)$.⁴ A plot of $N(\alpha) HG^*(j\omega)$ on a Nyquist diagram, and an investigation of this plot to determine its encirclements of the $-1 + j0$ point, will yield information as to the stability of the system. In Figure 2, the system that has a response given by curve (a) is stable, while the system with a response like curve (b) is unstable. There is occasionally some difficulty in determining if the plot encircles the $-1 + j0$ point; however, most books on control systems and servomechanisms outline the method for this investigation, and will not be given here.⁵

⁴H. Nyquist, "Regeneration Theory," Bell System Technical Journal, 11 (1932), pp. 126-47.

⁵G. J. Thaler and R. G. Brown, Servomechanism Analysis (New York, 1953), pp. 159-162.

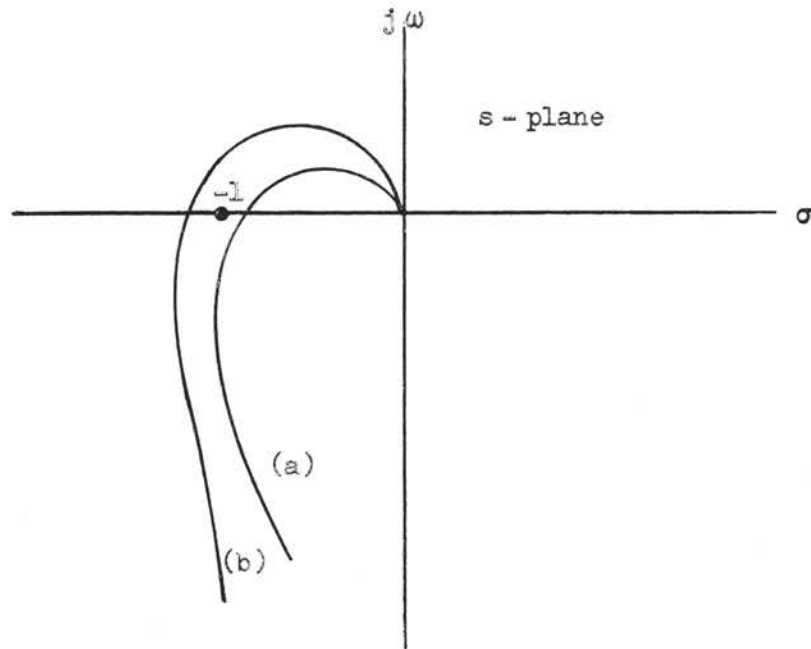


Figure 2. Nyquist Diagram

Another very important aspect of the Nyquist diagram is that not only absolute stability, but also the relative stability, of a system can be obtained. This is accomplished by observing the frequency phase plot in the neighborhood of the critical point. The system became more oscillatory as the plot is shifted to the left. Thus, the response of the system shown by curve (b), in Figure 3, is more oscillatory than the one shown by curve (a). Both systems are stable, however. The degree of instability of a system can be determined in the same way as the degree of stability. The system with a response shown by curve (c), in Figure 3, is not as unstable as the one with the response shown by curve (d).

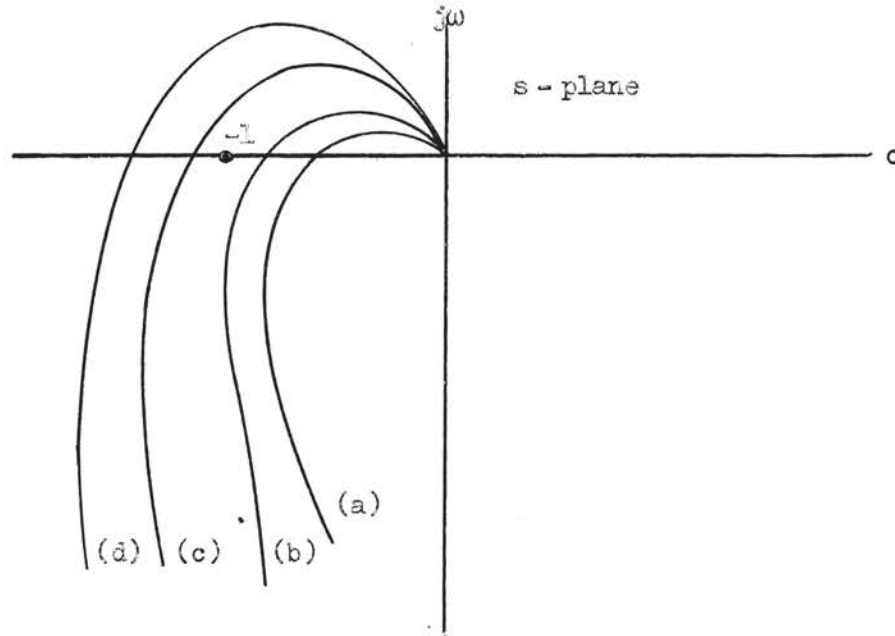


Figure 3. Stable and Unstable Plots on a Nyquist Diagram

A means of measuring the degree of stability or instability of a system has been set up through the use of M-circles. These circles are drawn on a Nyquist diagram and represent a constant magnitude of the output of the system to the input. This ratio is given as

$$M = \left| \frac{C^*(s)}{R^*(s)} \right| = \left| \frac{G^*(s)}{1 + HG^*(s)} \right| . \quad (10)$$

The locus of a constant magnitude ratio, M , may be shown to be a circle on the complex plane, with a radius

$$r = \frac{M}{M^2 - 1} , \quad (11)$$

and a center located at the point

$$\left[-\frac{M^2}{M^2 - 1}, 0 \right]. \quad (12)$$

A family of these constant magnitude circles may be drawn on the $HG^*(s)$ -plane and the degree of stability of the system is associated with the value of M which is tangent to the frequency phase plot. A system with a frequency phase plot tangent to the circle with M equal to 1.3, usually is considered satisfactory from the stability standpoint. Systems tend to be more oscillatory with higher values of M . A family of M -circles and a frequency phase plot are shown in Figure 4. The value of maximum M is 1.5.

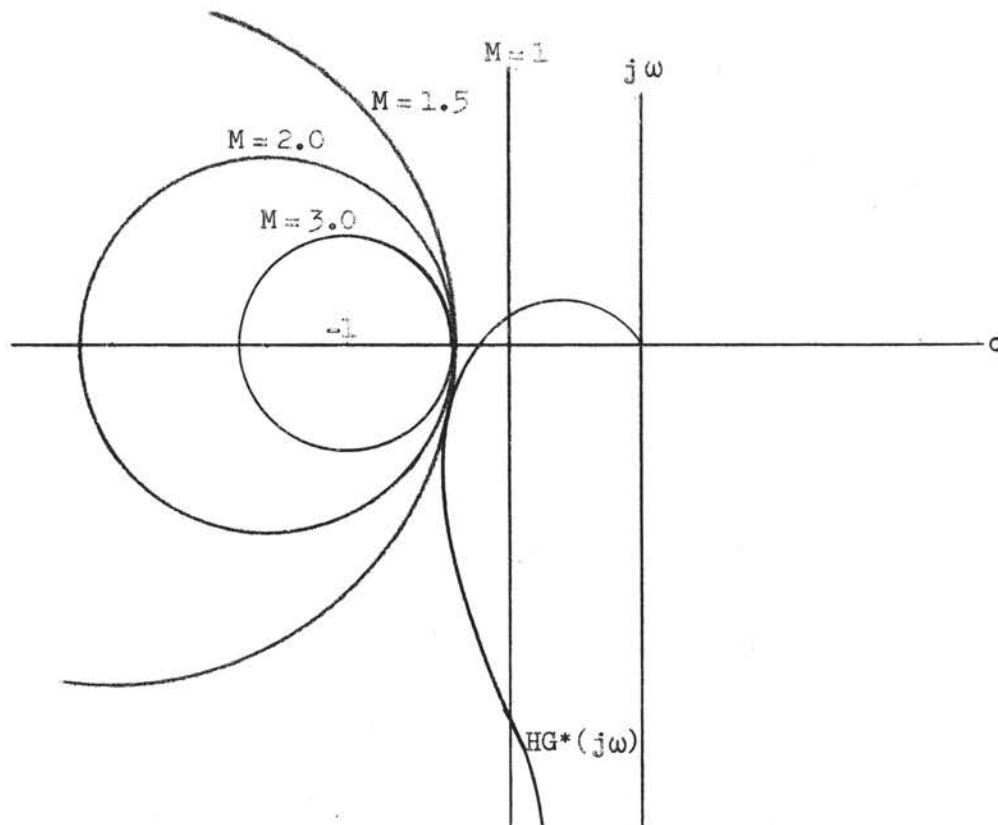


Figure 4. M -Circles and Frequency Phase Plot

It has been shown that the relative stability of a control system can be found by making a frequency phase plot of $N(\alpha) HG^*(s)$ on a Nyquist diagram. The analysis of the stability is performed by conventional methods of continuous-data linear systems once the plot is complete. The problem left to be performed in this thesis will be the one of obtaining the plot for $N(\alpha) HG^*(s)$. The subsequent chapters will be devoted to this problem.

CHAPTER III

ANALYTICAL STUDY

It was pointed out in Chapter II that the stability of a nonlinear sampled-data control system could be found from the frequency phase plot of $N(\alpha) HG^*(j\omega)$. It was also pointed out that the relative stability of the system, as well as the absolute stability, could be determined by this method. However, here are several problems which make it impossible to proceed immediately with the phase plot by conventional methods given in linear continuous-data systems. First, there is the problem of finding a way to express the nonlinear element, $N(\alpha)$. The second problem is one of obtaining the transfer function for $HG^*(j\omega)$, and the third problem is that of getting the composite response of $N(\alpha)$ and $HG^*(j\omega)$.

In this paper a method for obtaining the frequency phase plot of $N(\alpha) HG^*(j\omega)$ is reported. The study is limited to systems which have nonlinear elements of the "fast nonlinearity" type, and a control system which has only one sampler. The steps presented for obtaining the frequency phase plot for $N(\alpha) HG^*(j\omega)$ are: (1) plot $HG^*(j\omega)$ on a Nyquist diagram using methods developed for linear sampled-data control systems, (2) approximate $N(\alpha)$

by means of a "describing function", and (3) vary $HG^*(j\omega)$ in a manner that will account for the nonlinear element by using the approximation for $N(\alpha)$. The results of this will be an approximation for the frequency phase plot of $N(\alpha) HG^*(j\omega)$. This approximation for the frequency phase plot will in most cases yield satisfactory results for determining the relative stability of a nonlinear sampled-data control system. In those cases where the results are not satisfactory, a method for improving the frequency phase plot of $N(\alpha) HG^*(j\omega)$ is presented so that any degree of accuracy may be obtained.

Frequency Phase Plot for $HG^*(j\omega)$

The first step to be performed in obtaining a frequency phase plot for $N(\alpha) HG^*(j\omega)$ is to plot $HG^*(j\omega)$ on a Nyquist diagram in a manner which has been outlined in books on linear sampled-data control systems. The basic steps for obtaining the frequency phase plot for $HG^*(j\omega)$ are presented here in order to tie this portion of the method for obtaining the Nyquist plot for $N(\alpha) HG^*(j\omega)$ in with the second portion, which is on the approximation for the nonlinear element, $N(\alpha)$.

The method used for obtaining a Nyquist plot for $HG^*(j\omega)$ can best be shown by first observing the effect of a sampler on a signal, and then using this information to construct a frequency phase plot for the linear portion of the system. Once the characteristics of this sampler are

determined the remainder of the system can be described and analyzed in the usual manner. The sampler, along with its input and output, is shown in Figure 5. The sampler converts the continuous signal into a train of pulses, which are regularly spaced and have a magnitude equal to the function value at the sampling instant. Since the sampling duration is small compared to the time constants of the system, the output from the sampler can be considered as a train of impulses with the dimension representing the value of the continuous signal at the sampled instant. The output from the sampler can be written as:

$$x^*(t) = \delta(t) x(t), \quad (13)$$

where $\delta(t)$ is a train of impulses occurring every T seconds. T is called the sampling period. If the Laplace transform of Equation 13 is taken, the results will be

$$X^*(s) = \frac{1}{T} \sum_{n=-\infty}^{\infty} X(s + jn\omega_s), \quad (14)$$

where ω_s is the sampling frequency. Equation 14 places in evidence the effect of the sampler on a signal in terms of the frequency spectrum of the input and output. The most important characteristic of the sampler is the periodicity. $X^*(s)$ is a simple periodic function with a period $j\omega_s$. Figure 6 illustrates that $X^*(s)$ takes on the same value at congruent points (a_0, a_1, a_{-1} , etc.) in the various period strips in the s -plane.

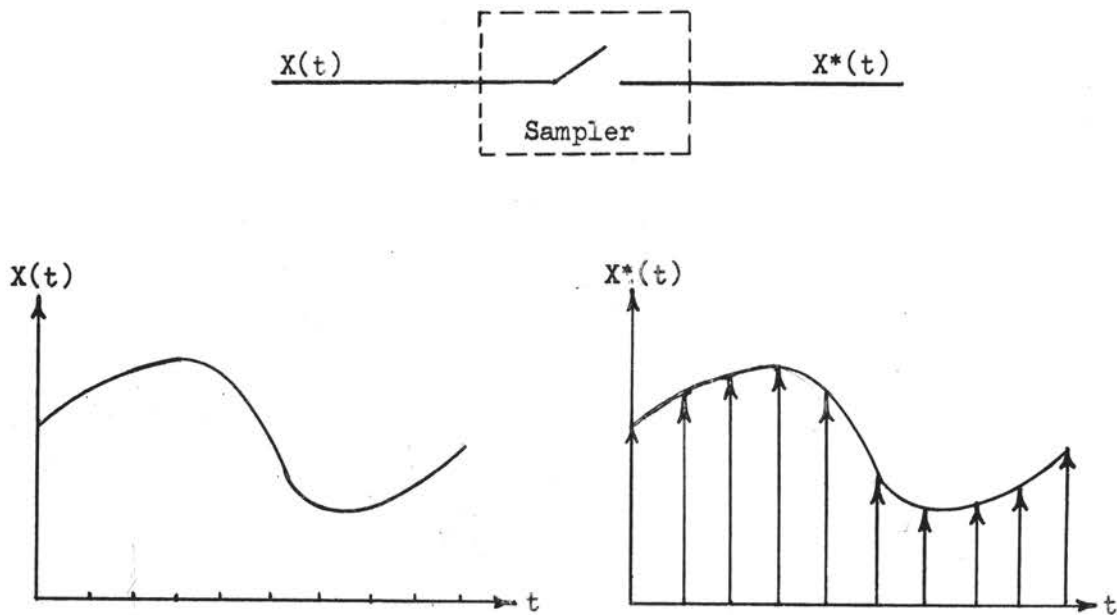


Figure 5. The Sampler and Waveforms of Input and Output

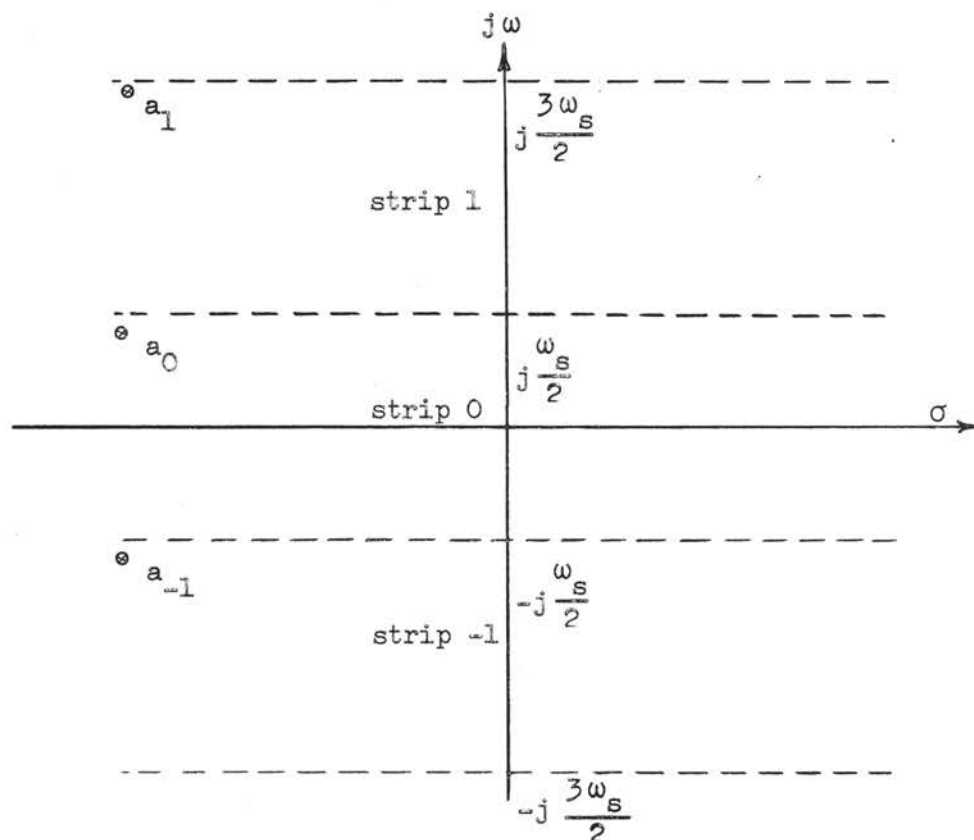


Figure 6. Periodicity Strips of $X^*(s)$ in the s -Plane

The periodicity property of $X^*(s)$ is also demonstrated by the frequency spectra plotted in Figure 7. Here the spectra of the sampler input is given in Figure 7a, and the frequency spectra of the sampler output, which was determined from Equation 14, is shown in Figure 7b. The sampler output consists of the spectrum of the primary signal and the spectra of the complementary signals. The spectrum of the primary signal is similar to that of the sampler input, except that it is attenuated by a factor $1/T$, and it is centered at zero frequency. The spectra of the complementary signals are identical with those of the primary signal, but they are displaced from the primary component by $n\omega_s$ units.

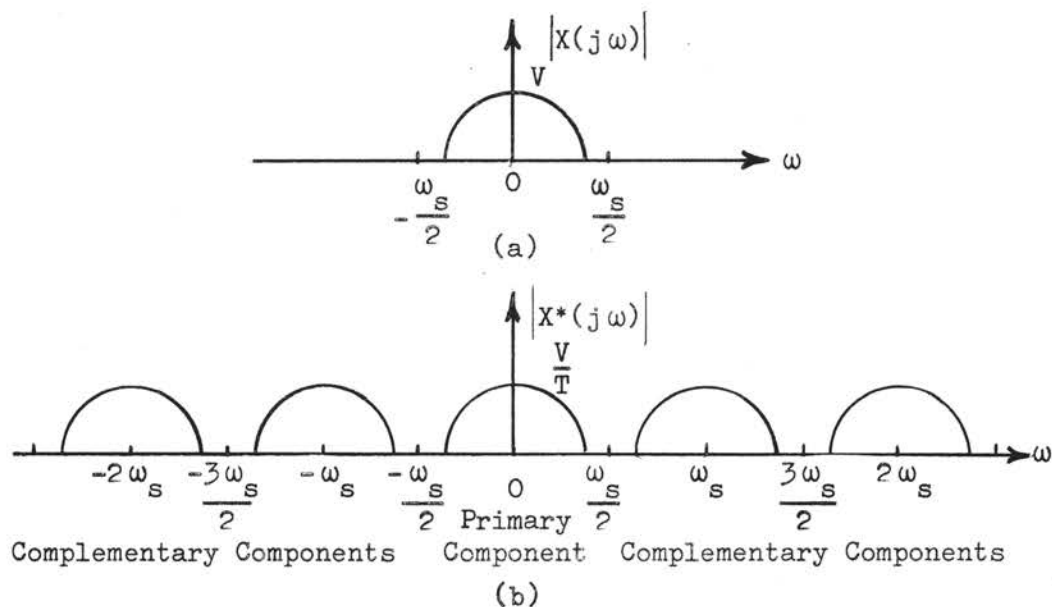


Figure 7. Frequency Spectra of the Original and the Sampled Signal

The primary component is the desired signal, and can generally be removed by filtering the unwanted complementary components. This filtering is possible if the sampling frequency is more than twice the highest frequency of the input signal. If the sampling frequency is decreased to less than twice the highest frequency of the input signal, distortion appears due to the entangled combination of the upper part of the primary component and the lower part of the first higher group of the complementary components. This is shown in Figure 8. Thus, signals of frequency equal to $\omega_s/2$ or higher cannot be transmitted by the sampling device. If it were desired to transmit signals of higher frequencies, the sampling rate of the system would have to be increased.

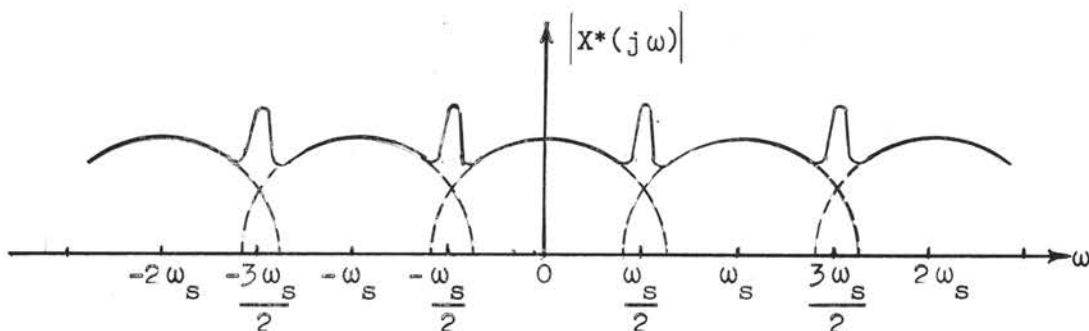


Figure 8. Frequency Spectrum of Sampler Output When Sampling Frequency is Less Than Twice the Highest Input Signal

The important thing to observe here is the periodicity introduced by the sampler, and that when $HG^*(s)$ is substituted in Equation 14 for $X^*(s)$ the result is

$$HG^*(s) = \frac{1}{T} \sum_{n=-\infty}^{\infty} HG(s + jn\omega_s) . \quad (15)$$

Equation 15 is the one that will be needed in this study.

The frequency phase plot of $HG^*(s)$ can be constructed by replacing the complex variable s with $j\omega$ and allowing ω to vary from minus infinity to plus infinity. If the right side of Equation 15 is expanded into the series

$$\begin{aligned} \frac{1}{T} \sum_{n=-\infty}^{\infty} HG(j\omega + jn\omega_s) &= \frac{1}{T} [HG(j\omega) + HG(j\omega + j\omega_s) + \\ &+ HG(j\omega + j2\omega_s) + \dots + HG(j\omega - j\omega_s) + \\ &+ HG(j\omega - j2\omega_s) + \dots], \end{aligned} \quad (16)$$

the frequency loci is the vectorial sum of each phasor, where the phasor represents a term of the series.

Since $HG^*(j\omega)$ is a periodic function with a period of $j\omega_s$, the frequency phase plot repeats itself when the frequency is increased by ω_s . Thus, the polar plot of $HG^*(j\omega)$ for the frequency range from minus infinity to plus infinity is identical with that for the frequency range 0 to ω_s . Furthermore, since the polar plot of $HG^*(j\omega)$ is symmetrical with respect to the real axis, the plot for the

frequency range between $\omega_s/2$ and ω_s is the mirror image of the plot for the frequency range between 0 and $\omega_s/2$. As a result, in investigating the frequency phase characteristics of a sampled-data system only the frequency range from 0 to $\omega_s/2$ is of interest.

When constructing the Nyquist diagram, it is usually possible to limit the computation to a small number of the phasors of Equation 16. The number of phasors needed depends upon the bandwidth of the system and can be seen in the construction process. When the sampling frequency ω_s is high in comparison with the bandwidth of the system, Equation 16 can be approximated by the first three terms of the series without much loss of accuracy. Thus, Equation 16 becomes

$$\frac{1}{T} \sum_{n=-\infty}^{\infty} HG(j\omega + jn\omega_s) \approx \frac{1}{T} HG(j\omega) + \frac{1}{T} HG(j\omega - j\omega_s) + \frac{1}{T} HG(j\omega + j\omega_s). \quad (17)$$

The first term of the right-hand member of Equation 17 is the predominating term, the second term is the major correction term, and the third term is added for obtaining better accuracy. In order for the approximation of $HG^*(j\omega)$ by a few terms of the series given in Equation 16 to be effective, it is necessary for $HG(j\omega)$ to approach zero at least as rapidly as $1/\omega^2$ for frequencies above ω_s .¹

¹J. R. Raggazzini, and G. F. Franklin, Sampled-Data Control Systems (New York, 1958), p. 131.

The construction process for the polar plot is explained in Figure 9. First the polar plot of $T^{-1}HG(j\omega)$ is constructed for both positive and negative frequencies, then the three phasors, $T^{-1}HG(j\omega_1)$, $T^{-1}HG(j\omega_1 - j\omega_s)$, and $T^{-1}HG(j\omega_1 + j\omega_s)$, are added vectorially to give the approximate value of $T^{-1}HG^*(j\omega_1)$. $T^{-1}HG(j\omega_1)$ is given in Figure 9 by phasor OA, $T^{-1}HG(j\omega_1 - j\omega_s)$ by OB, and $T^{-1}HG(j\omega_1 + j\omega_s)$ by OC. The three phasors add together vectorially to produce OE. OE is the approximate value of the frequency phase plot of a linear sampled-data system when the frequency ω_1 is applied to the input. Additional points along the frequency phase plot may be found in this same manner at ω_2 , ω_3 , etc. When enough of these points have been determined, the results will be the frequency phase plot of the linear sampled-data control system. This is shown by the dotted line in Figure 9.

Approximation for the Nonlinear Element

The method for obtaining a frequency phase plot for the linear sampled-data control system has been presented, thus the attention now turns to the problem of finding a way to express the transfer function of the nonlinear element, $N(\alpha)$, and combining that transfer function with $HG^*(j\omega)$. As stated earlier, the nonlinear elements which are represented by $N(\alpha)$ in this thesis are of the type known as "fast nonlinearities"; that is, types in which the mode of operation of the system changes rapidly

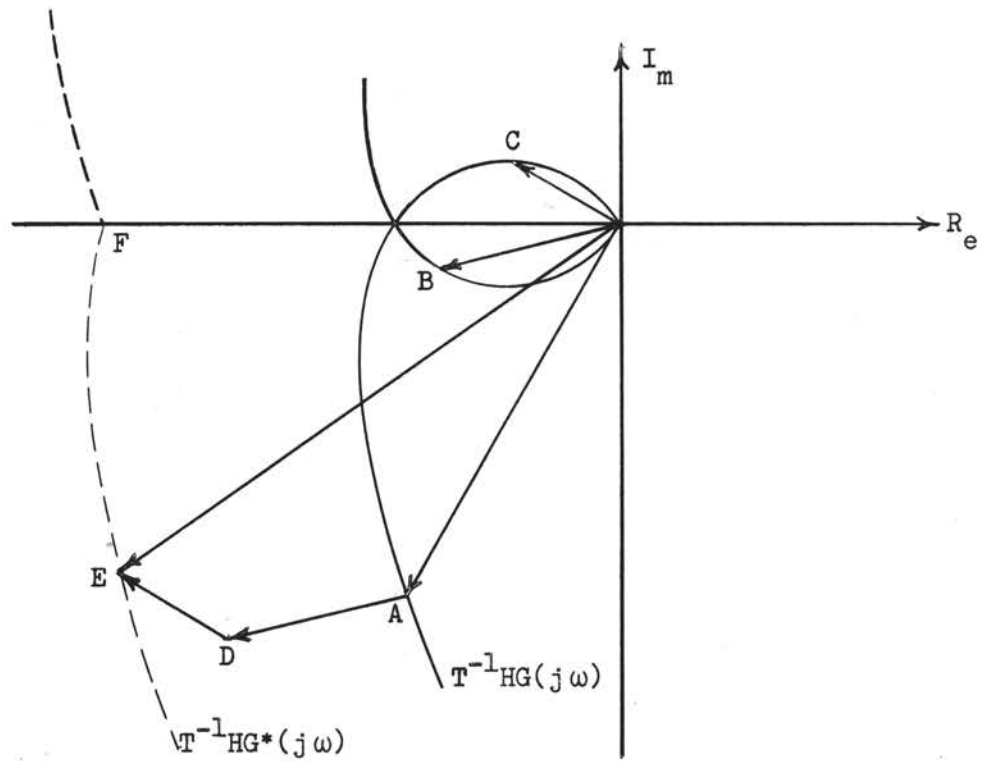


Figure 9. Construction of the Frequency Phase Plot for $HG^*(j\omega)$

compared to its response time. Some nonlinearities of this type are saturation, hysteresis or backlash, and dead zone. The input-output characteristics of these are shown in Figure 10.

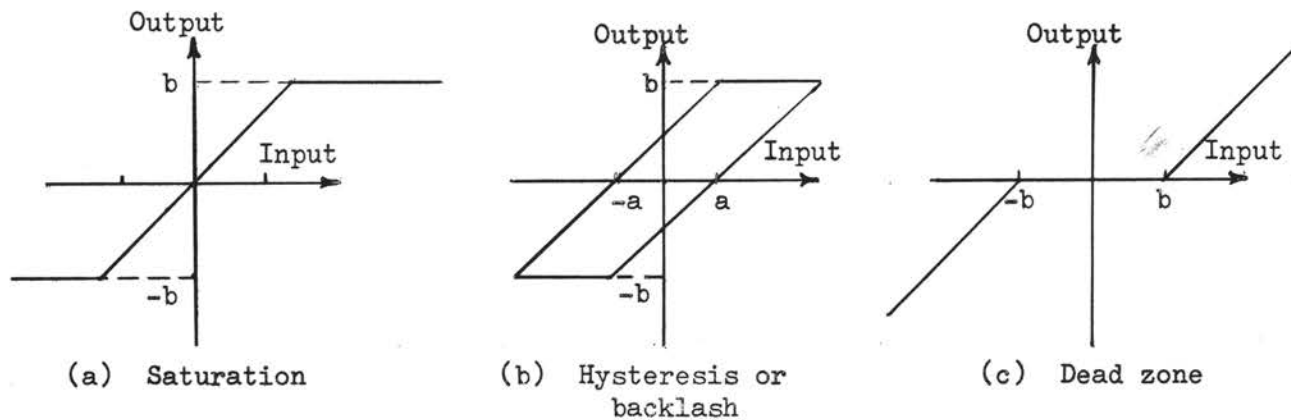


Figure 10. Input-Output Characteristics of Nonlinear Elements

In the study of nonlinear continuous-data systems a method known as the "describing-function" is used quite extensively to represent the element $N(\alpha)$.² The describing-function will be introduced here as a first approximation for $N(\alpha)$, and this value will be used to obtain the frequency phase plot for $N(\alpha) HG^*(j\omega)$.

²J. G. Truxal, Automatic Feedback Control System Synthesis (New York, 1959), p. 134.

The describing-function analysis is based on three assumptions: (1) There is only one nonlinear element in the system. If there is more than one, then a single element will be considered as containing all the nonlinearities of the system. It is theoretically possible to consider systems with more than one isolated nonlinearity, but the analysis becomes unduly complicated. (2) The output of the nonlinear element depends only on the present value and past history of the input. In other words, no time-varying characteristics are included in $N(\alpha)$. (3) If the input of $N(\alpha)$ is a sinusoidal signal, only the fundamental component of the output of $N(\alpha)$ contributes to the input to the system.

The last assumption is the key to the describing-function analysis, and it is justified on two grounds; first, the harmonics of the output of $N(\alpha)$ are ordinarily of smaller amplitude than the fundamental; and second, in most feedback control systems, the gain of the system transfer function decreases as the frequency increases, with the result that the higher harmonics are attenuated more than the fundamental in the transmission through the system.

The describing-function is defined as the ratio of the fundamental component of the output to the amplitude of the input. Thus, if the input to the element, $N(\alpha)$, is $e = e_1 \sin \omega t$ and the Fourier series analysis gives the output as $d = d_1 \sin(\omega t + \theta_1) + d_3 \sin(3\omega t + \theta_3) + \dots$, then the

describing-function would be given by

$$N(\alpha) = \frac{d_1}{e_1} \angle \theta_1 , \quad (18)$$

where θ_1 is the phase shift between the input wave and the fundamental wave, and α is the variable used to indicate the degree of nonlinearity in the element. Actually the describing-function is a method for linearizing the non-linear element. A change in α will change the value of $N(\alpha)$, which is given in Equation 18.

The value given for $N(\alpha)$ in Equation 18 is considered to be the transfer function of $N(\alpha)$ and used to adjust the frequency phase plot of $HG^*(j\omega)$, which was shown in Figure 9 (page 23). This adjustment is made by multiplying $HG^*(j\omega)$ by $\frac{d_1}{e_1} \angle \theta_1$ for all values of ω . The resulting plot for $\omega = \omega_1$ will be

$$\left[|HG^*(j\omega_1)| \angle \theta_L \right] \left[\frac{d_1}{e_1} \angle \theta_1 \right] .$$

This equals

$$\left| HG^*(j\omega_1) \right| \left| \frac{d_1}{e_1} \right| \angle \theta_L + \theta_1 ,$$

or it can be seen that the plot of $HG^*(j\omega)$ can be multiplied by $\frac{d_1}{e_1}$ and shifted in phase by θ_1 . In cases where θ_1 varies as ω varies, the value of θ_1 must be changed for each value of ω . The resulting plot on a Nyquist diagram will be the frequency phase plot of $N(\alpha) HG^*(j\omega)$. With this plot the examination of the degree of stability of

the nonlinear sampled-data control system can be carried out by the conventional methods used in linear continuous-data systems.

Improved Approximation for $N(\alpha)$ $HG^*(j\omega)$

The describing-function is only an approximation for the transfer function of $N(\alpha)$. In many instances, this approximation is adequate because the higher order harmonics are usually relatively small when compared to the fundamental and also the linear portion of the control system usually tends to filter out the higher order harmonics. As the harmonics become large when compared to the fundamental, the frequency phase plot of $N(\alpha) HG^*(j\omega)$, using the describing-function to represent $N(\alpha)$, becomes less accurate. The ratio of the next higher harmonic and the fundamental is a measure of the accuracy of the describing-function analysis. Since this ratio is a measurement of the accuracy of the frequency phase plot for $N(\alpha) HG^*(j\omega)$, it appears that the ratio of the harmonic to the fundamental could be used to improve the accuracy of the frequency phase plot. The scheme used in this thesis to obtain the first correction to the frequency phase plot which was obtained using the describing-function was to find the percentage of the magnitude of a given harmonic to the magnitude of the fundamental. This percentage was multiplied by the value of the linear sampled-data frequency phase plot taken at the frequency of the harmonic.

This value is then added vectorially to the value of the frequency phase plot at the fundamental frequency. In other words, if it is desired to obtain the effect of the third harmonic on the frequency phase plot at the frequency ω_a , and the magnitude of the third harmonic is five per cent of the fundamental, then the process is to take five per cent of the magnitude of the linear sampled-data frequency plot at the frequency $3\omega_a$ and add that value vectorially to the sum of the response for the system to the fundamental at ω_a and the second harmonic at $2\omega_a$. The sum of these three phasors is the value of frequency phase plot at the frequency, ω_a , when all higher-order harmonics to be considered in the above manner depend only on the degree of accuracy desired.

Example of the Method

The method of obtaining the frequency phase plot of $N(\alpha) HG^*(j\omega)$ can be explained best by means of an illustration. The nonlinear element to be used in the example will be saturation. The input-output characteristics of this type nonlinear element was shown in Figure 10a (page 24). When the input to the element is sinusoidal, then the output wave will be as shown in Figure 11. The symbol α is the angle and b is the magnitude at which saturation occurs. The Fourier series of this output wave is given as

$$y = y_1 \sin(x + \alpha_1) + y_3 \sin(3x + \alpha_3) + \dots , \quad (19)$$

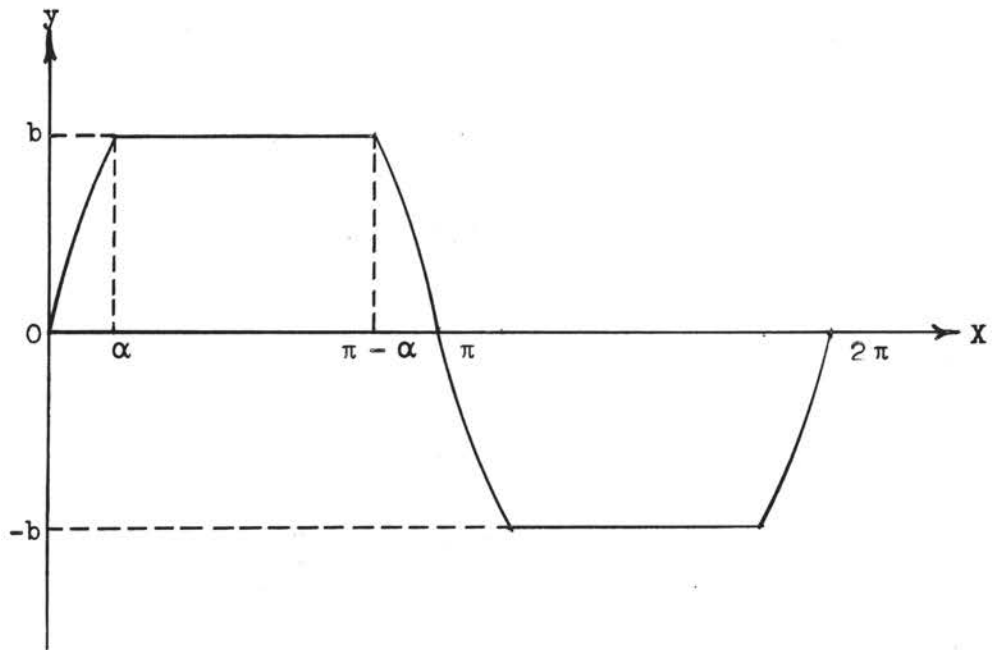


Figure 11. Output of Saturation Type Nonlinearity
With Sinusoidal Input

when the input is $e = a \sin x$. The values of y_n can be found from

$$y_n = \frac{2}{\pi} \int_0^{\pi} e \sin nx \, dx \quad n = 1, 3, 5, \dots \quad (20)$$

where

$$e = a \sin x \quad 0 < x < \alpha, \quad (21)$$

$$e = a \sin \alpha \quad \alpha < x < \pi - \alpha, \quad (22)$$

and

$$e = a \sin x \quad \pi - \alpha < x < \pi. \quad (23)$$

The evaluation for y_1 becomes

$$y_1 = \frac{2}{\pi} \left[\int_0^{\alpha} a \sin x \sin x \, dx + \int_{\alpha}^{\pi - \alpha} a \sin \alpha \sin x \, dx + \int_{\pi - \alpha}^{\pi} a \sin x \sin x \, dx \right], \quad (24)$$

which yields

$$y_1 = \frac{2a}{\pi} \left[\alpha + \frac{1}{2} \sin 2\alpha \right], \text{ where } 0 < \alpha < \frac{\pi}{2}. \quad (25)$$

Thus, when $\alpha = \frac{\pi}{2}$ (no saturation) the value for $y_1 = a$, which is the magnitude of the input, and at $\alpha = 0$ the value for $y_1 = 0$. The describing function for the saturation-type nonlinearity is given as the fundamental component divided by the input signal, which is

$$N(\alpha) = \frac{y_1}{a} \angle \alpha_1 = \frac{2}{\pi} \left[\alpha + \frac{1}{2} \sin 2\alpha \right] \angle 0^\circ, \quad 0 < \alpha < \frac{\pi}{2}. \quad (26)$$

There is no phase shift between the input and output signal, thus $\alpha_1 = 0$ for all values of α ; however, this is not true for all types of nonlinearities.

The describing function for the saturation type nonlinearity has been obtained in Equation 26, therefore, the first step in the analysis is to plot $HG^*(j\omega)$, the linear frequency phase plot of the sampled-data system, on the Nyquist diagram. This is accomplished by the conventional method that was described earlier, where $HG^*(j\omega)$ was approximated with the vector sum of the first three terms of the series

$$HG^*(j\omega) = \frac{1}{T} HG(j\omega) + \frac{1}{T} HG(j\omega - j\omega_s) + \frac{1}{T} HG(j\omega + j\omega_s). \quad (27)$$

The next step is to replace $N(\alpha)$ with the describing function. The describing function can be considered as a first approximation for $N(\alpha)$. In the case of the saturation nonlinearity, the describing function is a reduction in magnitude only, without shift in phase. Thus, once a value of α has been selected (that is, a certain amount of saturation is present), the value of $HG^*(j\omega)$ can be reduced in magnitude by the amount of the describing function. The effect of the nonlinear element, therefore, tends to move the plot of the frequency phase to the right, and since the critical point is the point $-1 + j0$, the degree of stability of the system will be increased.

The method just described may be seen in Figure 12 where the value of the describing function is assumed to be approximately one-half. The point A is the magnitude and phase for the linear frequency phase locus at ω_a , while the point A' is the corresponding magnitude and phase for the frequency phase locus for the nonlinear system, $N(\alpha) HG^*(j\omega_a)$. This same reduction is carried out at B and B', C and C', etc., until the plot for $N(\alpha) HG^*(j\omega)$ is complete for all values of frequency between 0 and $\omega_s/2$.

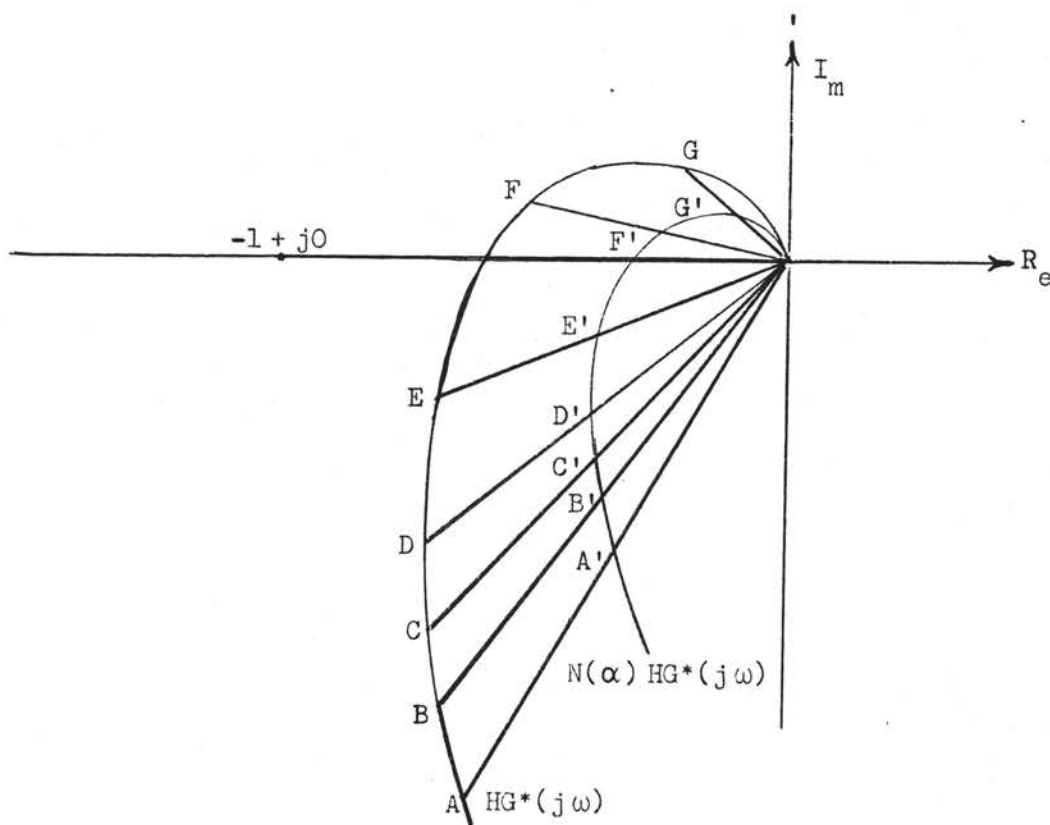


Figure 12. Method for Constructing the Nonlinear Sampled-Data Frequency Phase Loci

The control engineer may be curious to know if the plot of $N(\alpha) HG^*(j\omega)$ obtained by using the describing function is adequate to yield desired results, therefore, the next problem which he must take into account is the one of knowing when it is necessary to consider higher-order harmonics. Perhaps one of the best ways to find out how important the higher-order harmonics are, in comparison to the fundamental, is to make a plot of the fundamental and several of the harmonics as the variable is varied. From this plot the control engineer should be able to see very clearly the relationship between the fundamental and the other harmonics. Figure 13 is a plot of the magnitudes of the fundamental, third, and fifth harmonics for a saturation-type nonlinearity, as the angle α is varied from 0° to 90° . The symbol α is the angle associated with the amount of saturation present and can be expressed as

$$\alpha = \sin^{-1} \left[\frac{\text{Magnitude of saturation}}{\text{Magnitude of input signal}} \right]. \quad (28)$$

When no saturation is present, the magnitude of saturation is equal to the magnitude of the input signal and $\alpha = 90^\circ$; and at the other extreme, when the system is completely saturated and the magnitude of saturation is zero, $\alpha = 0^\circ$. Referring to Figure 13, one can see that, as the amount of saturation increases, or as α decreases, the magnitude of the third harmonic relative to the magnitude of the fundamental increases at a rapid rate. Thus, for slight

saturation ($\alpha > 60^\circ$), the percentage of third harmonic to fundamental is less than about five per cent. For values of saturation in the region $60^\circ < \alpha < 90^\circ$, the value for $N(\alpha)$ can be approximated very well by using only the fundamental harmonic; however, for values of $\alpha < 60^\circ$ the third harmonic must be taken into account in order to have an approximation for $N(\alpha)$ that is within five per cent of the actual value. At values of $\alpha < 30^\circ$, the fifth harmonic becomes noticeable and should also be taken into consideration.

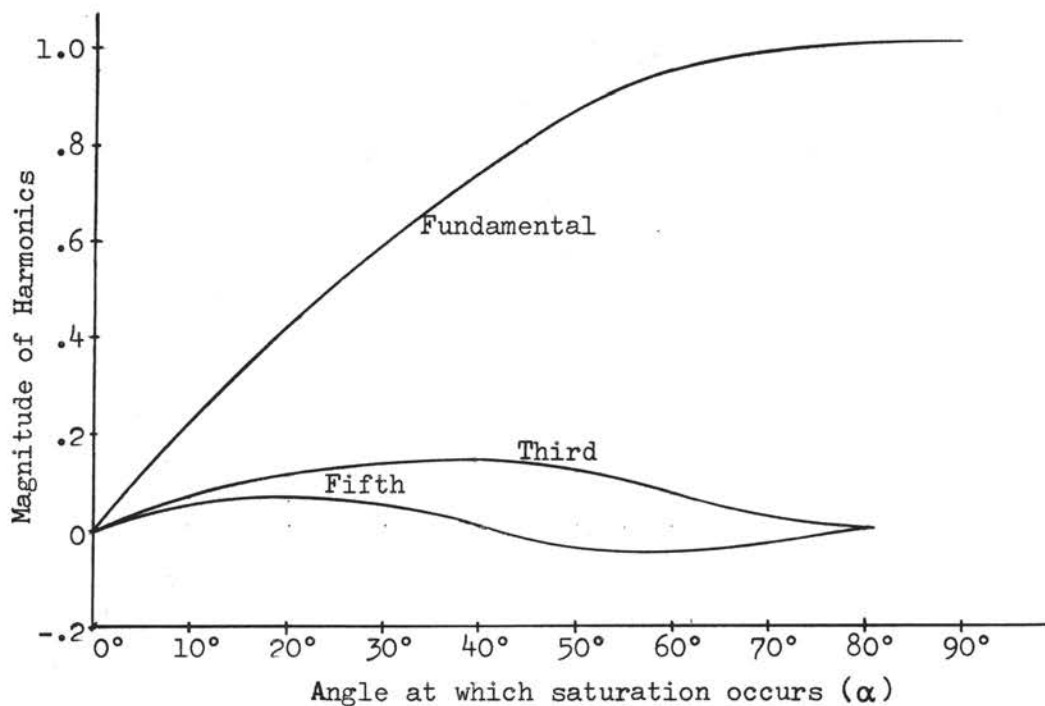


Figure 13. Magnitude of Harmonics for Saturated Sine Wave

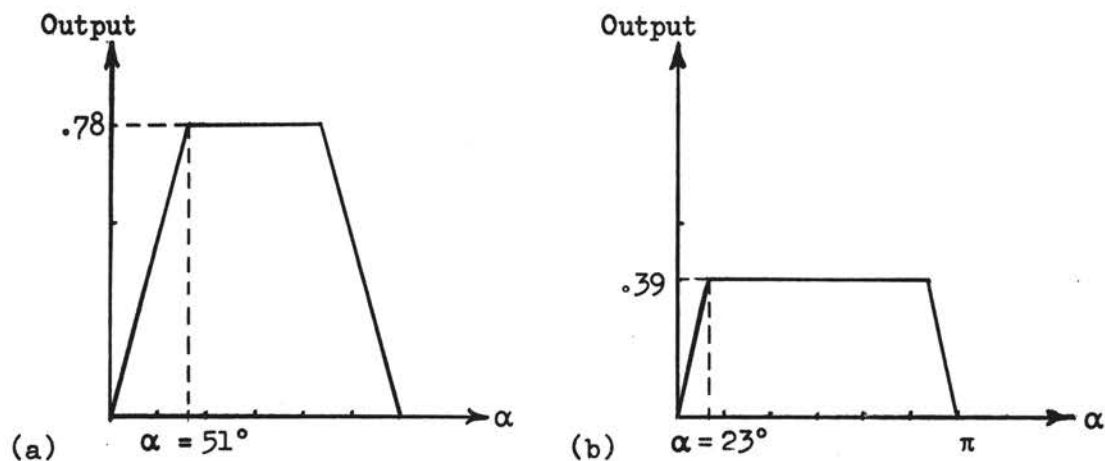


Figure 14. Two Degrees of Saturation

The two waveforms shown in Figure 14 illustrate why the higher-order harmonics must be compared with the fundamental in order to have any meaning in the calculation of the effect of the higher-order harmonics. One can see that the period and magnitude of the input wave to the nonlinear element is the same for both waves, but the output waves are completely different. In Figure 14a, the wave is saturated when $\alpha = 51^\circ$, and in Figure 14b, the wave is saturated when $\alpha = 23^\circ$. Referring now to Figure 13, one finds that the magnitude of the fundamental and third harmonics have the values listed in Table I.

From Table I, one can see that the magnitudes of the third harmonic, at each value of α , are approximately the same when compared to the input wave. However, one also can see that the third harmonic has a much greater effect on the wave shown in Figure 14b than the one shown in

Figure 14a. If one would compare the third to the fundamental harmonic, one would find that the percentage of third harmonic to fundamental would be considerably different. This is tabulated in Table II.

TABLE I

RELATIVE MAGNITUDES OF THE FUNDAMENTAL
AND THIRD HARMONICS FOR TWO DEGREES
OF SATURATION

α	51°	23°
Fundamental	.88	.48
Third	.09	.13

TABLE II

PERCENTAGE THIRD HARMONIC FOR TWO DEGREES
OF SATURATION

α	51°	23°
% third harmonic	10	27

The information given in Tables I and II will now be used to illustrate how it can be used to determine the stability of the nonlinear sampled-data control system shown in Figure 15. It will be assumed that the nonlinear element is of the saturation-type which saturates at $\alpha = 23^\circ$. Thus, from Table I, the value of the fundamental is 0.48 of the input signal and from Table II the third harmonic is 27 per cent. This information will be used to complete the frequency phase plot of an actual system.

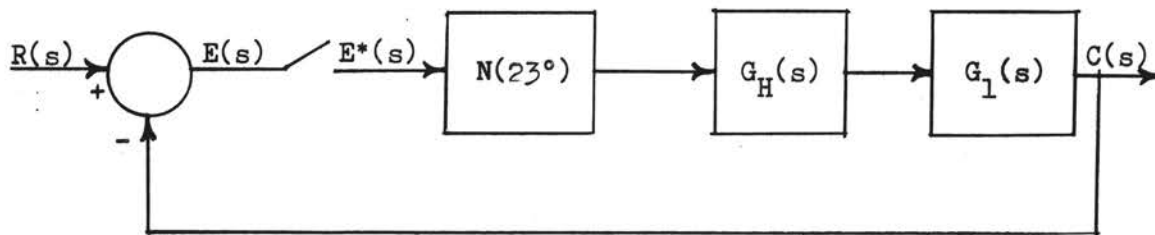


Figure 15. Nonlinear Sampled-Data Control System

The system to be controlled is $G_1(s) = \frac{40}{s(.05s + 1)}$, the sampling frequency, f_s , is 20 cycles per second, and the transfer function designated by $G_H(s)$ is a hold circuit. The hold circuit is a low-pass filter which removes the complementary signal components that were produced by the sampler. This is needed in order to reduce the ripple in the output signal of the sampled-data

control system. One of the simplest holding devices is the zero-order holding circuit or boxcar generator, in which the value of the input pulse is held constant until the arrival of the next sampling pulse. The waveforms of the input and output of a zero-order holding circuit are shown in Figure 16.

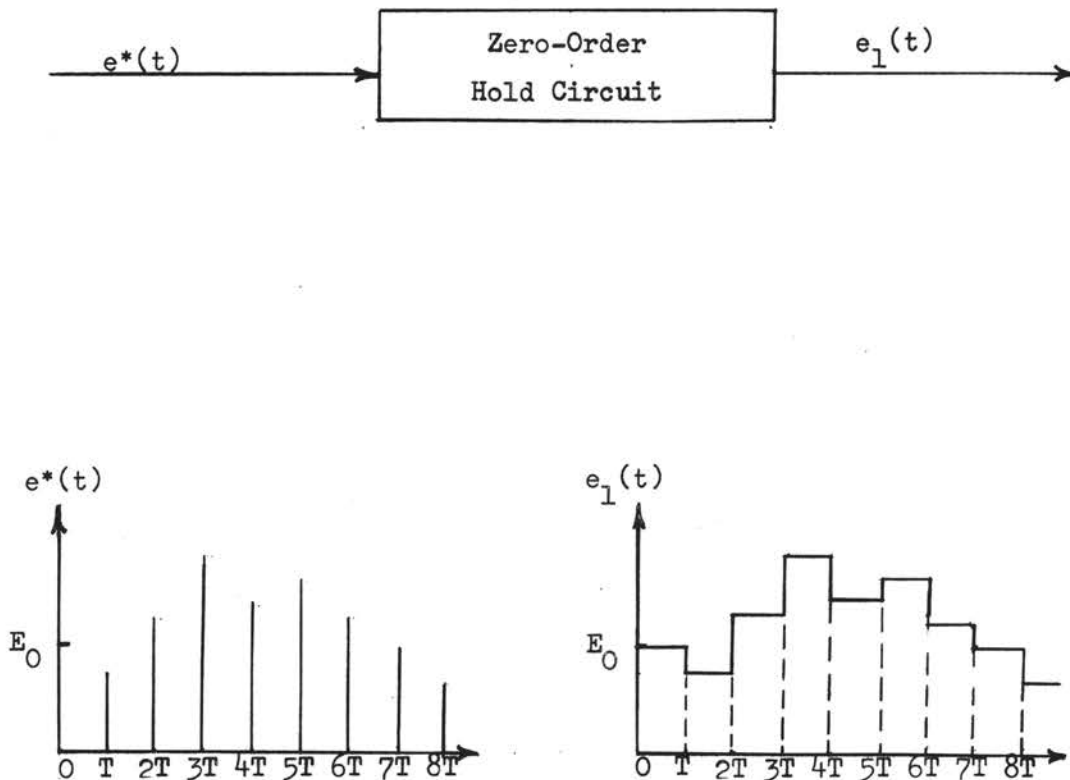


Figure 16. Waveforms at the Input and Output of a Zero-Order Hold Circuit

The transfer function of the zero-order hold circuit was given by Tou as

$$G_H(s) = \frac{1 - \epsilon^{-Ts}}{s}, \quad (29)$$

where T is the period of the sampling rate.³ Thus, the over-all transfer function of the system shown in Figure 15 is given as

$$G(s) = G_H(s) G_1(s), \quad (30)$$

or

$$G(s) = \frac{40(1 - \epsilon)^{-Ts}}{s^2(.05s + 1)}. \quad (31)$$

The first step of the analysis is to calculate the continuous-data open-loop response of $G(j\omega)$ as ω is varied from zero to infinity. This has been calculated and tabulated in Column II of Table III. The second step in the calculation is to find the linear sampled-data system response. This is calculated using the first two terms of Equation 27, and multiplying the quantity by T in order to account for the hold circuit. These values are tabulated in Column VI of Table III, and plotted as curve (a) in Figure 17.

The third step in the calculation is the one used to adjust the linear sampled-data frequency phase plot in such a manner as to account for the fundamental harmonic. This is accomplished by multiplying each value of the

³J. T. Tou, Digital and Sampled-Data Control Systems (New York, 1959), p. 134.

TABLE III

CALCULATED OPEN-LOOP RESPONSE OF THE NONLINEAR SAMPLED-DATA CONTROL SYSTEM

I	II	III	IV	V	VI	VII	VIII	IX
f	$G(j\omega)$	$G(j\omega - j\omega_s)$	$\sum_{n=-1}^0 G(j\omega + jn\omega_s)$	$TG_H(j\omega)$	$G^*(j\omega)$	$.48G^*(j\omega)$	$.27G^*(j3\omega)$	$N(23^\circ)G^*(j\omega)$
1.5	<u>3.84/-115°</u>	<u>.06/170°</u>	<u>3.87/-116°</u>	<u>.99/- 14°</u>	<u>3.83/-130°</u>	<u>1.84/-130°</u>	<u>.20/-193°</u>	<u>1.92/-135°</u>
2	<u>2.68/-123°</u>	<u>.06/170°</u>	<u>2.72/-125°</u>	<u>.98/- 18°</u>	<u>2.68/-143°</u>	<u>1.29/-143°</u>	<u>.14/-214°</u>	<u>1.34/-149°</u>
3	<u>1.55/-133°</u>	<u>.07/170°</u>	<u>1.60/-135°</u>	<u>.96/- 27°</u>	<u>1.54/-162°</u>	<u>.74/-162°</u>	<u>.08/-250°</u>	<u>.75/-170°</u>
4	<u>.99/-142°</u>	<u>.08/169°</u>	<u>1.05/-146°</u>	<u>.94/- 36°</u>	<u>.99/-182°</u>	<u>.48/-182°</u>	<u>.06/-299°</u>	<u>.47/-189°</u>
6	<u>.50/-152°</u>	<u>.10/167°</u>	<u>.58/-160°</u>	<u>.86/- 54°</u>	<u>.50/-214°</u>	<u>.24/-214°</u>	<u>.11/-397°</u>	<u>.13/-212°</u>
8	<u>.30/-158°</u>	<u>.14/165°</u>	<u>.43/-170°</u>	<u>.76/- 72°</u>	<u>.33/-242°</u>	<u>.16/-242°</u>		
10	<u>.20/-163°</u>	<u>.20/163°</u>	<u>.40/-180°</u>	<u>.64/- 90°</u>	<u>.26/-270°</u>	<u>.12/-270°</u>		
12	<u>.14/-165°</u>	<u>.30/159°</u>	<u>.43/-190°</u>	<u>.51/-108°</u>	<u>.22/-299°</u>	<u>.11/-299°</u>		
14	<u>.10/-167°</u>	<u>.50/152°</u>	<u>.58/-200°</u>	<u>.37/-126°</u>	<u>.21/-328°</u>	<u>.10/-328°</u>		

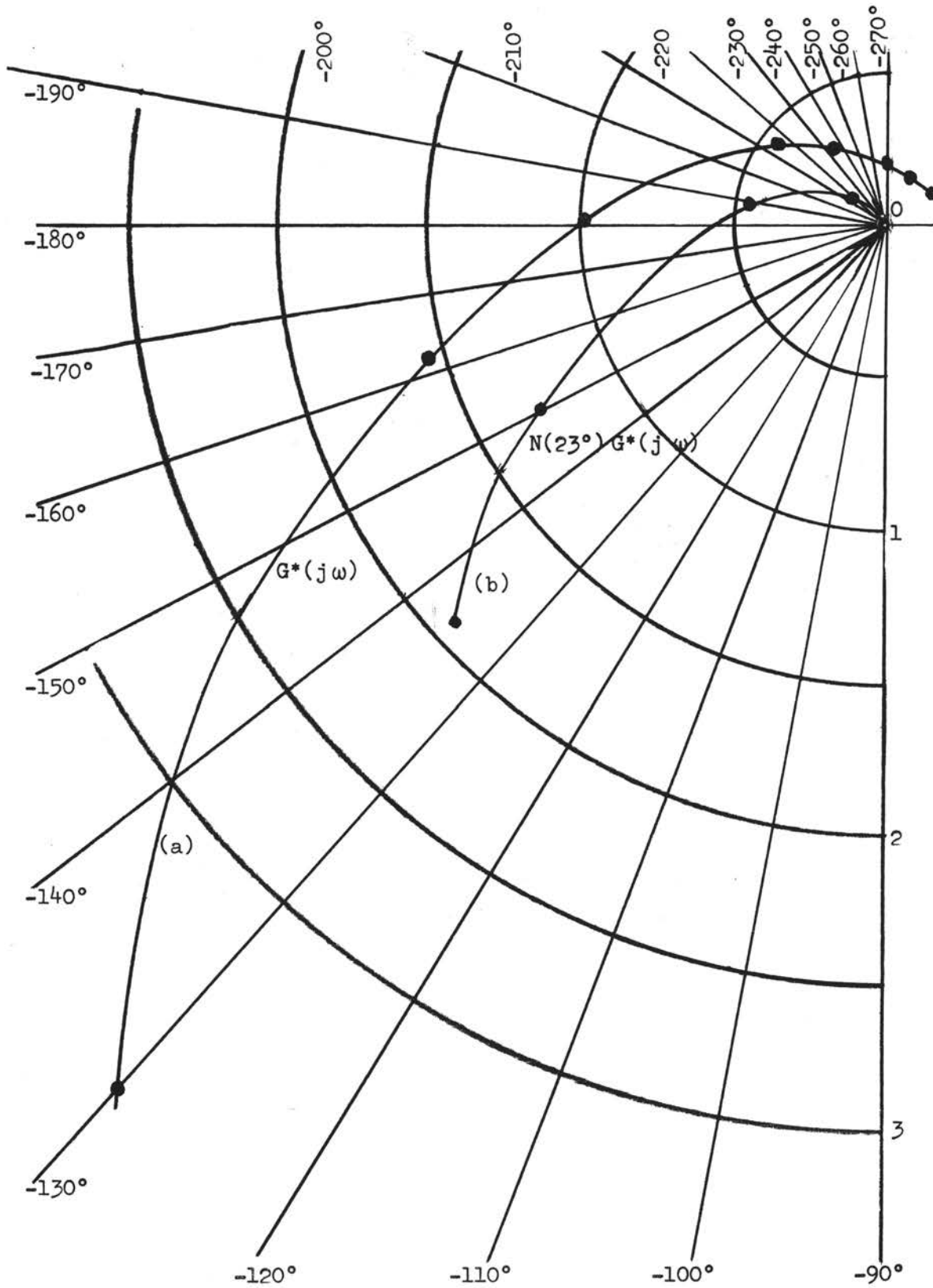


Figure 17. Frequency Characteristic of the Nonlinear Sampled-Data Control System

linear frequency phase by the value of the fundamental harmonic when $\alpha = 23^\circ$. This value of the fundamental is 0.48. The result of this is listed in Column VII of Table III; it is the first approximation for the frequency phase plot of the nonlinear sampled-data system. The final step in the calculation is used to obtain a better approximation for the frequency phase plot. This calculation is carried out by adding vectorially 27 per cent of the linear sampled-data locus at $3\omega_a$ to the value of the first approximation at ω_a . This final result is tabulated in Column IX of Table III, and is the desired frequency characteristic of the nonlinear sampled-data control system. A plot of this is shown as curve (b) in Figure 17.

The actual steps used to obtain the frequency phase plot, as shown by curve (b) in Figure 17, were:

1. Obtain a frequency phase plot of the linear continuous-data system $HG(j\omega)$.
2. Obtain the frequency phase plot of the linear sampled-data system $HG^*(j\omega)$.
3. Obtain the describing function for $N(\alpha)$ and multiply that value by $HG^*(j\omega)$. This yields the first approximation for the frequency phase plot of the nonlinear sampled-data control system.
4. In the case where higher accuracy is desired, each higher ordered harmonic from the output of the nonlinear element is compared to the

fundamental as a percentage. This percentage is multiplied by the linear sampled-data system response at $n\omega_a$, where n is the value of the harmonic under consideration, and ω_a is the value of ω where a point on the frequency phase plot of $N(\alpha) HG^*(j\omega)$ is being calculated. The value of the percentage of the higher ordered harmonic multiplied by the linear sampled-data system response at $n\omega_a$ is added vectorially to the results obtained at ω_a in 3 (on preceding page). This step is repeated until enough points along the plot have been obtained so that a smooth curve can be approximated.

CHAPTER IV

EXPERIMENTAL STUDY

In Chapter III an analysis was made to determine the polar plot of the open-loop transfer function of a nonlinear sampled-data control system. In order to verify the results given in that chapter, an experimental study was conducted using a Donner electronic analog computer to simulate the control system. This chapter will be a discussion of the system used in the study, the method used to obtain the results, and the tabulation of the results. The analysis of the results will be given in Chapter V.

The system chosen in this experimental study is shown in Figure 15. The transfer function of the controlled system was given as $G_1(s) = \frac{40}{s(.05s + 1)}$; the transfer function of the hold circuit was $G_H(s) = \frac{1 - e^{-Ts}}{s}$; the sampling frequency, f_s , was equal to 20 cycles per second, and the nonlinear element was a saturation-type nonlinearity which has an input-output characteristic as shown in Figure 10a (page 24). Data were obtained for three values of saturation; that is, for three values of α . The values of α equal to 90° , 51° , and 23° were taken and recorded.

System Used for the Study

The transfer function of $G(s) = \frac{40(1 - e^{-.05s})}{s^2(.05s + 1)}$ was programmed on a Donner electronic analog computer using the techniques given by Johnson.¹ The analog computer circuit for this transfer function is shown in Figure 18.

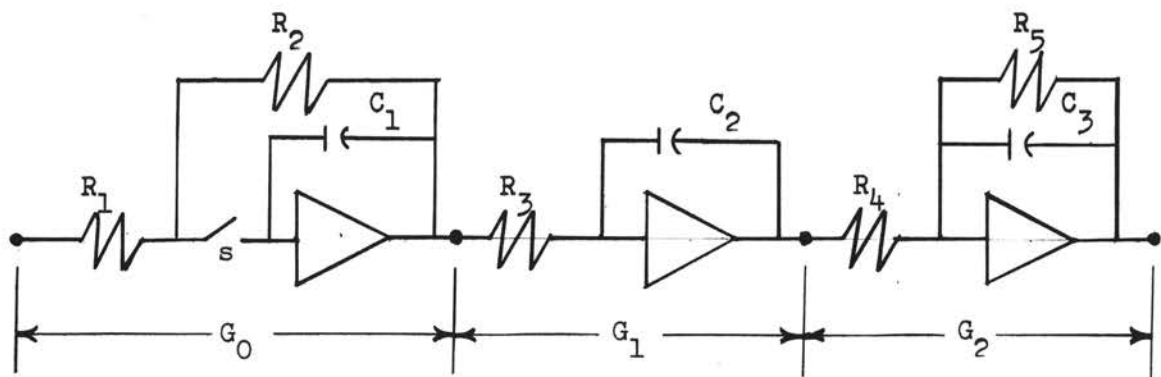


Figure 18. Analog Computer Circuit for Forward Transfer Function

The transfer function of each of the amplifiers shown in Figure 18 are

$$G_0 = \frac{1 - e^{-.05s}}{s}, \quad (32)$$

$$G_1 = \frac{1}{R_3 C_2 s}, \quad (33)$$

¹C. L. Johnson, Analog Computer Techniques (New York, 1956).

and

$$G_2 = \frac{R_5/R_4}{R_5 C_3 s + 1} \cdot \quad (34)$$

Thus, the over-all open-loop transfer function is

$$G = G_0 G_1 G_2 \quad (35)$$

or

$$G = \frac{(R_5/R_2 R_4 C_2) (1 - e^{-.05s})}{s^2 (R_5 C_3 s + 1)} \cdot \quad (36)$$

The sampler was simulated by a relay, which closed for one-fifth of a cycle when its coil was energized. A Hewlett-Packard sine wave oscillator was used to energize the relay at 20 cycles per second.

The saturation-type nonlinearity was produced with a diode circuit used in conjunction with one of the operational amplifiers of the Donner electronic analog computer. The circuit for performing this operation is shown in Figure 19 along with the input and output waveforms to the circuit.

The output wave is identical to the input wave, with the exception of the clipping of the upper portion of the wave, which is the effect of saturation in a system. The potentiometers were used to adjust the amount of clipping.

A schematic of the complete system as used in this study is shown in Figure 20.

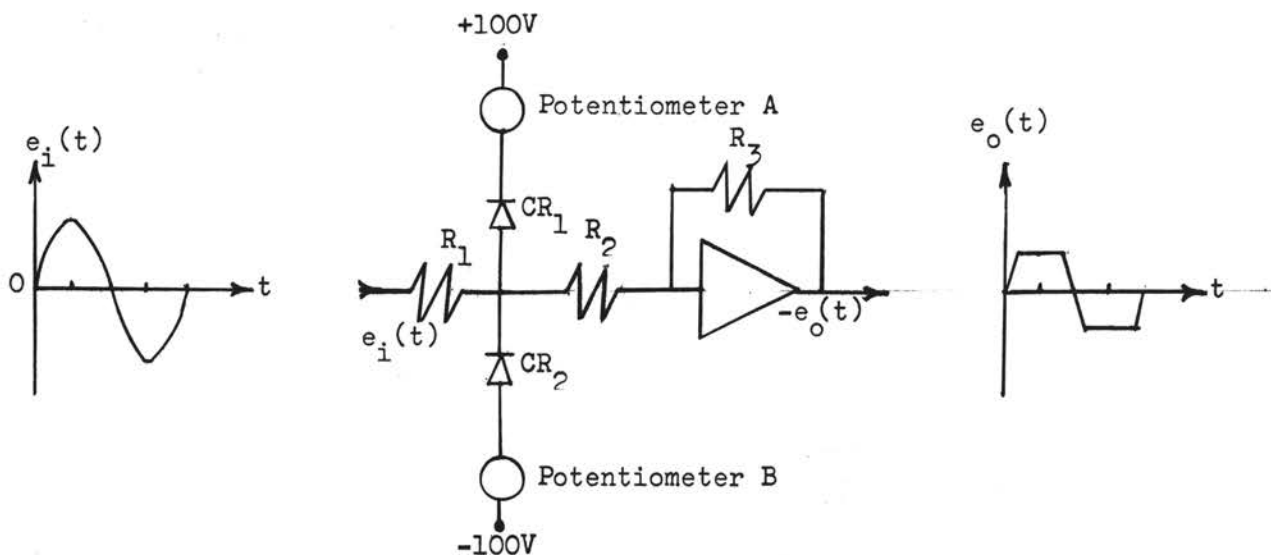


Figure 19. Circuit for Generating Nonlinearity
Along With Input and Output Waveforms

Method Used to Obtain Results

The procedure used to obtain the results was to set up the system shown in Figure 20 on the Donner electronic analog computer. A sine wave of 20 cycles per second from the sine wave oscillator was applied to the coil of the relay, and the amplitude of the wave was adjusted until the contacts of the relay were closed for approximately one-fifth of the period (0.05 second). The next step was to apply a sine wave of variable frequency to the input designated by $r(t)$; the amplitude of this signal was varied until it produced an actuating signal $e(t)$ of a specific magnitude, which in turn produced the desired amount of

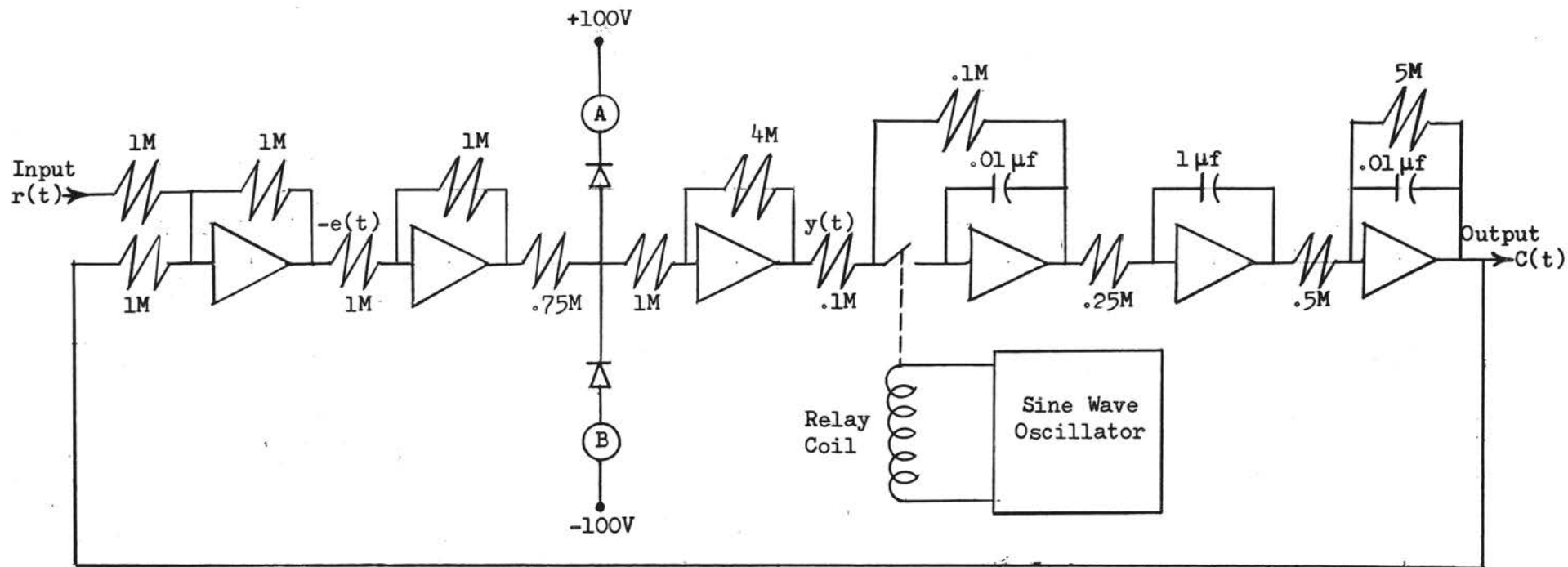


Figure 20. Analog Computer Schematic of the Nonlinear Sampled-Data Control System

nonlinearity. With this specific magnitude of signal $e(t)$, the two potentiometers A and B were adjusted until the output $y(t)$ was limited to the desired value. Thus, when the signal $e(t)$ was adjusted to have the magnitude specified above, the saturation was set at one particular value. As the frequency at the input of the system, $r(t)$, was varied, its magnitude had to be adjusted to bring $e(t)$ to the desired value.

A Hewlett-Packard oscilloscope was used to measure the peak-to-peak voltage $c(t)$ at the output, and the actuating signal $e(t)$. Also with the aid of an electronic switch, the two signals, $c(t)$ and $e(t)$, were displayed on the oscilloscope at the same time in order to measure the phase relationship of the two waves. With this information, the open-loop response of the system could be calculated by the equation

$$G(j\omega) = \frac{c(j\omega)}{e(j\omega)} \underline{\text{ / phase angle between } c \text{ and } e}. \quad (37)$$

These data were taken for the three case $\alpha = 90^\circ$ (linear system), $\alpha = 51^\circ$ (small amount of nonlinearity), and $\alpha = 23^\circ$ (large amount of nonlinearity).

Results Obtained From the Experimental Analysis

The data tabulated in Table IV are the results obtained with the saturation of the system fixed at three different levels. The second column is the data for α equal to 90° (no saturation or linear). The third column

TABLE IV
EXPERIMENTAL RESULTS

f	$N(90^\circ)G^*(j\omega)$	$N(51^\circ)G^*(j\omega)$	$N(23^\circ)G^*(j\omega)$
1.73	3.20/ <u>-128°</u>	2.90/ <u>-130°</u>	1.60/ <u>-131°</u>
2.00	2.80/ <u>-131°</u>	2.40/ <u>-133°</u>	1.40/ <u>-134°</u>
2.35	2.04/ <u>-138°</u>	1.92/ <u>-140°</u>	1.05/ <u>-142°</u>
2.53	1.96/ <u>-141°</u>	1.76/ <u>-143°</u>	0.97/ <u>-144°</u>
2.94	1.56/ <u>-144°</u>	1.36/ <u>-146°</u>	0.75/ <u>-152°</u>
3.90	0.96/ <u>-157°</u>	0.84/ <u>-164°</u>	0.45/ <u>-166°</u>
5.00	0.64/ <u>-180°</u>	0.60/ <u>-180°</u>	0.30/ <u>-180°</u>
5.90	0.44/ <u>-193°</u>	0.34/ <u>-185°</u>	0.10/ <u>-185°</u>

is for α equal to 51° (small amount of saturation), and the fourth column for α equal to 23° (large amount of saturation). The analysis of these experimental results will be presented in the next chapter.

CHAPTER V

SUMMARY AND ANALYSIS OF RESULTS

The purpose of this thesis was to present a method for obtaining the frequency phase plot of a nonlinear sampled-data control system so that the relative stability of the system could be determined. The nonlinear elements are of the "fast nonlinearity" type, or ones in which the mode of operation of the system changes rapidly compared to its response time. The analysis was carried out in the frequency domain and the Nyquist diagram was the tool used for determining the stability.

It was shown in Chapter II that the relative stability of a nonlinear sampled-data control system could be determined if the open-loop response of the system was plotted on a Nyquist diagram. It was also shown that once the frequency phase plot, or open-loop frequency response, had been obtained, the relative stability of the nonlinear sampled-data system could be found in the same manner as the relative stability of a linear continuous-data control system. That is, the relative stability of a nonlinear sampled-data control system could be obtained through the uses of M-circles in the same manner as they are used for studying stability in linear continuous-data systems.

There were a number of problems which had to be considered before the frequency phase plot could be constructed. The first problem was that of selecting a method for plotting $HG^*(j\omega)$, the sampled transfer function of the linear portion of the system. This problem was overcome by examining the effect of a sampler on a signal and noting that the output from the sampler can be expressed in the series

$$HG^*(j\omega) = \frac{1}{T} HG(j\omega) + \frac{1}{T} \sum_{n=1}^{\infty} HG(j\omega + jn\omega_s) + \frac{1}{T} \sum_{n=1}^{\infty} HG(j\omega - jn\omega_s). \quad (38)$$

Each of the terms on the right-hand side of Equation 38 can be represented by a vector, and the vectorial sum of these yield the value $HG^*(j\omega)$. The response $HG^*(j\omega)$ can usually be approximated very accurately by only a few terms of the series; therefore, the frequency phase plot of the linear portion of the system may be obtained without much difficulty.

The next problem which had to be overcome was finding a way to express or represent the nonlinear element or nonlinear portion of the system. The describing-function is a method used to represent these elements in continuous-data systems; therefore, a successful attempt was made to extend this method to sampled-data systems. The

describing-function is defined as the value of the fundamental harmonic at the output of the nonlinear element, divided by the value of the input signal. This is expressed in a formula as

$$N(\alpha) = \frac{d_1}{e_1} \angle \theta_1, \quad (39)$$

where θ_1 is the angle between the two, d_1 is magnitude of the fundamental harmonic, e_1 is the magnitude of the input signal and α represents the degree or amount of nonlinearity.

The magnitude and phase of the describing-function is used in the same manner as any transfer function; that is, Equation 39 is inserted into the system in the place of the nonlinear element.

Equation 39 is a very good approximation for the transfer function of the nonlinear element for a great number of control systems. This statement is true because the higher order harmonics are usually very small when compared to the fundamental, and also because the system usually attenuates the higher order harmonics. In cases where this is true, the describing-function is accurate enough for determining the relative stability of the system; however, there are times when the describing-function does not adequately describe the nonlinear element and the higher-order harmonics must be considered along with the fundamental if accurate results are required.

The higher-order harmonics were used to obtain a more accurate frequency phase plot in the following manner: First, the value of each of the more predominated harmonics was calculated using the Fourier series analysis, and this value was compared to the fundamental as a percentage. The value of this percentage was multiplied by the magnitude and phase of the linear response of the system at the frequency of the harmonic. The result obtained from this multiplication was added vectorially to the describing-function's response. The describing-function's response was taken at the frequency of the fundamental, and the harmonic responses were taken at the frequency of each harmonic. As an example, if it were desired to find the response of the nonlinear system at the frequency ω_a with third and fifth harmonics present, the procedure to be followed would be: (1) find the percentage of the third and fifth harmonic relative to the fundamental; (2) multiply the value of the percentage of third harmonic by the value of the linear response at $3\omega_a$ and the value of the percentage of fifth harmonic at the value of the linear response at $5\omega_a$; and (3) add vectorially both results obtained from (2) above to the vector which would be obtained when the magnitude and phase of the fundamental was multiplied by the linear frequency response at the frequency ω_a . The sum of these three vectors is the response of the nonlinear system at the frequency ω_a . It is assumed in this example that the effect of the harmonics above the fifth is negligible.

Analysis of the Results

The frequency phase plot of a typical nonlinear sampled-data control system, shown in Figure 15, was obtained in Chapter III. The techniques presented in this thesis were used to obtain this plot. The nonlinear element of the system was one which saturated at a value of α equal to 23° . The value of the fundamental at this degree of saturation was found, through a Fourier series analysis, to be 0.48. The percentage of the third harmonic, relative to the fundamental, was 27 per cent.

The linear frequency phase plot was calculated from the vector sum of the first two terms of the series

$$HG^*(j\omega) = \frac{1}{T} HG(j\omega) + \frac{1}{T} HG(j\omega - j\omega_s) + \frac{1}{T} HG(j\omega + j\omega_s) + \dots \quad (40)$$

Nine different values of ω were used in order to obtain a smooth curve on the Nyquist diagram. The results of this calculation are tabulated in Column VI of Table III, and a frequency phase plot is shown as curve (a) in Figure 17. This plot passes through or slightly to the left of the critical point $(-1 + j0)$; therefore, the linear system is unstable. Actually, the linear response was of little interest except that it was needed in the calculation for the nonlinear response.

The next step of the calculation was performed by multiplying each term of Column VI of Table III, the linear

frequency response, by 0.48, the magnitude of the fundamental harmonic. This result is tabulated in Column VII of Table III. The third step was performed by multiplying each term of the linear frequency response (Column VI of Table III) by 27 per cent, the percentage of the third harmonic. Column VII is a tabulation of this result. Each term in that column is 27 per cent of the linear frequency response at three times the frequency of the line in which it is located. That is, the second term from the top in Column VIII, which is located in the line corresponding to a frequency of 2 cycles per second, is $0.14/\underline{-214^\circ}$. This term is 27 per cent of the linear frequency response at a frequency of 6 cycles per second, which is the fifth term in Column VI.

The vector sum of Columns VII and VIII yields the results of the nonlinear frequency phase plot for the sampled-data system shown in Figure 15. These same results are plotted as curve (b) in Figure 17. The nonlinear system is stable and the degree of stability, or intersection of the frequency phase plot with a M-circle, is $M = 2.8$. Although the intention here was not to improve the stability of the system with the addition of a nonlinear element, the system was changed from an unstable one to one which is very stable. The objective was to present a method which would enable a control engineer to obtain a frequency phase plot of a nonlinear sampled-data control system, a plot from which he would be able to make a system stability

analysis using techniques already known to him.

An experimental study was conducted in order to verify the results obtained from the analytical study of Chapter III. Data were taken for three degrees of saturation; that is, for three values of α . The values of α were 90° , 51° , and 23° . The results from this experimental study are recorded in Table IV. The result obtained with α equal to 90° is the linear response of the system.

Although the system used in the experimental study was supposed to be an analog of the system used in the analytical study, it was found that the linear response of the two systems differed. This difference in the responses was due to the differences in the sampler and hold circuit used in the two studies. The output waveform from the sampler and hold circuit used in the analytical calculations is shown in Figure 21(a), and the waveform obtained from the experimental study is shown in Figure 21(b). The difference between the two waveforms was produced because the sampler used in the experimental study closed for a time period of $T/5$, whereas, the sampler in the analytical study was closed only momentarily. The sampler and hold circuit, like the one which produced the waveform in Figure 21b, will cause less phase shift in the sampled-data frequency response than a sampler and hold circuit with a waveform like that shown in Figure 21a. Therefore, the phase shift found in the experimental study was not as great as that calculated in the analytical study.

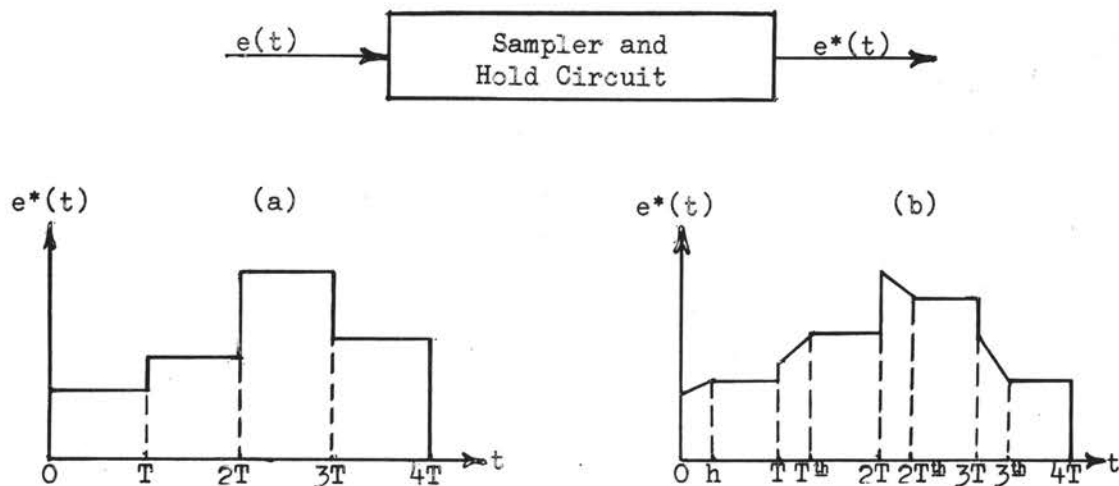


Figure 21. Output Waveforms From Sampler and Hold Circuit

Before a true comparison could be made between the experimental and analytical study, the analytical results had to be changed to take into account a sampler and hold circuit with a waveform of the type shown in Figure 21b. This change made the experimental system essentially identical to that used in the analytical study. The curve shown in Figure 22 is the corrected response of the system used in the analytical study, and the points which were obtained from the experimental study are plotted on the same curve. The experimental points are designated by the symbol \circ . It can be seen that the experimental points agree very well with the calculated curve.

The linear frequency phase plot, shown in Figure 22, was used to obtain calculated data for the plot of the nonlinear sampled-data system with α equal to 51° and 23° .

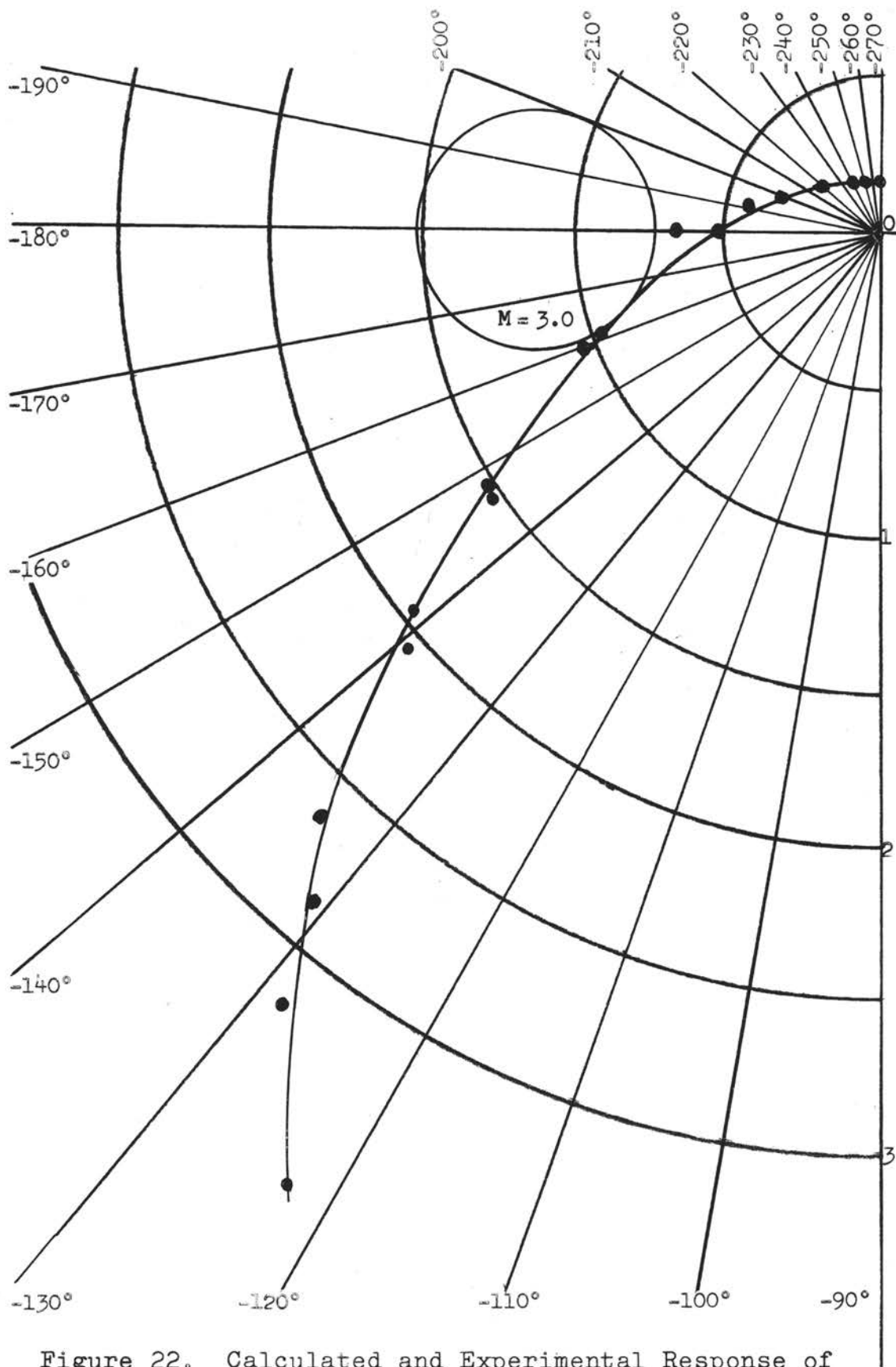


Figure 22. Calculated and Experimental Response of the Linear Sampled-Data Control System ($\alpha = 90^\circ$)

These two curves are shown in Figures 23 and 24, respectively. The results of the experimental data are plotted on each of these curves and designated by \circ . The experimental results again agree very well with the calculated results.

The degree of stability of each of the three saturated systems was determined by the employment of M-circles. It was found that the degree of stability increased with saturation. The change was from $M = 3$, for the linear system, to $M = 2.6$ for α equal 51° and to $M = 1.7$ for α equal 23° . From these results, it becomes apparent that a saturating type nonlinear element could be used to improve the stability of a system.

Some difficulty was experienced in determining the phase shift between the input and output waves to the system at input signal near one-half the sampling frequency. This was due to subharmonic generation within the system brought about by the nonlinearity. Because of this difficulty and because the system would seldom be operated in the region of $\omega_s/2$, no special effort was made to obtain these results.

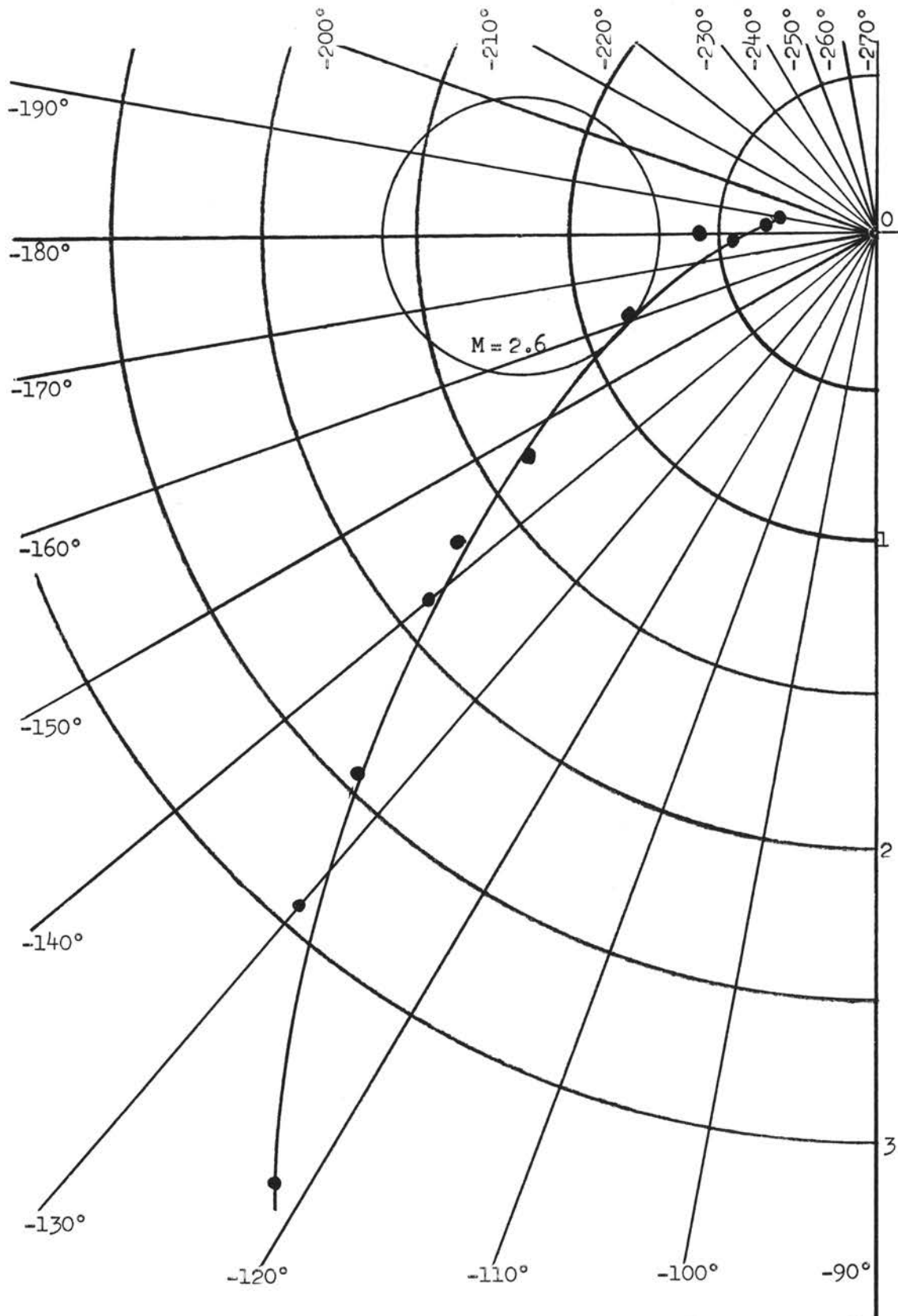


Figure 23. Calculated and Experimental Response of the Nonlinear Sampled-Data Control System ($\alpha = 51^\circ$)

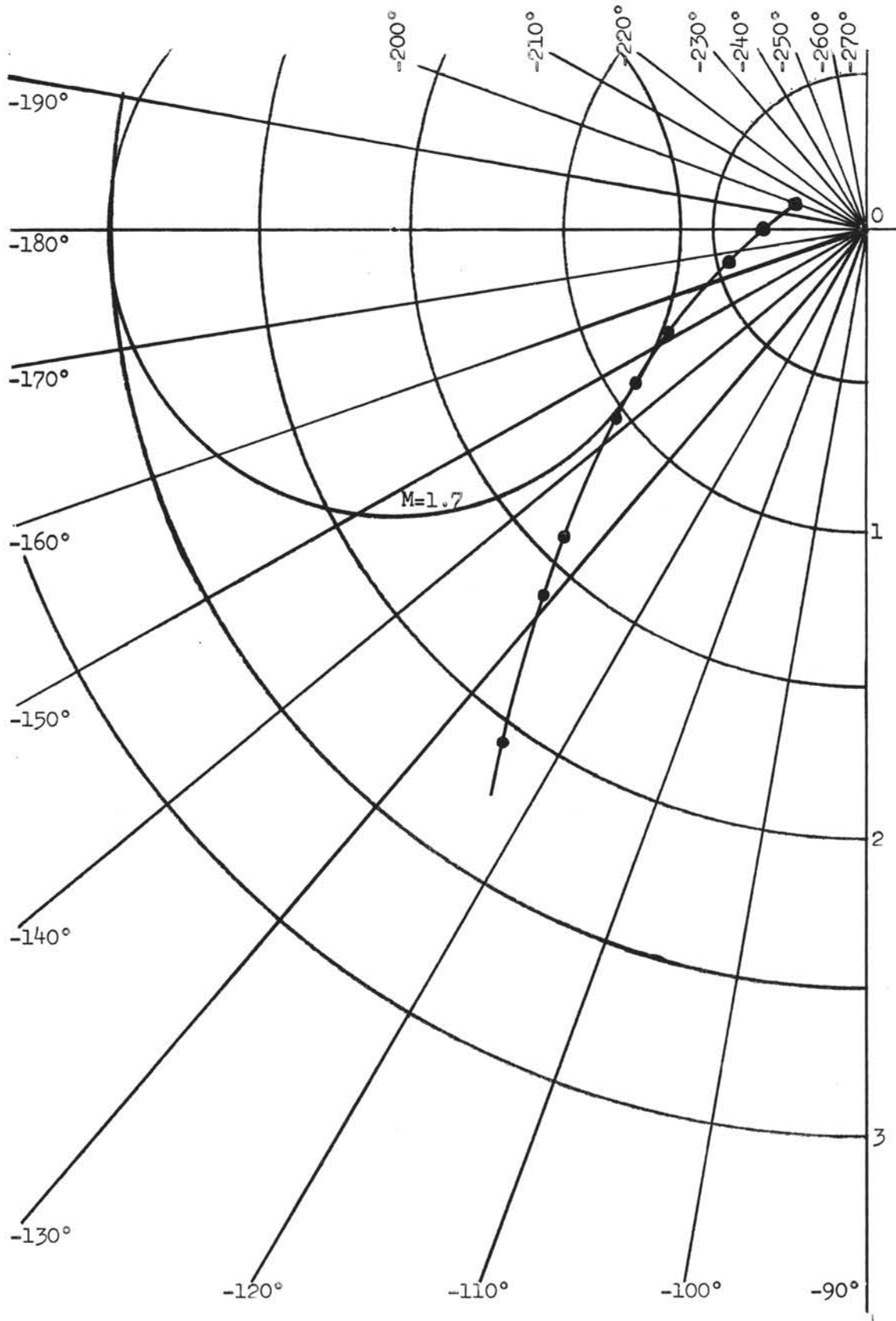


Figure 24. Calculated and Experimental Response of the Nonlinear Sampled-Data Control System ($\alpha = 23^\circ$)

CHAPTER VI

CONCLUSIONS

It was the object of this thesis to study the stability of nonlinear sampled-data control systems using the real frequency domain. The graphical tool used to study stability was the Nyquist diagram. The nonlinear elements of the system are of the fast nonlinearity-type in which the mode of operation of the system changes rapidly compared to its response time. Nonlinear elements of this type are saturation, hysteresis or backlash, dead zone, etc. As a result of this study, a technique has been developed for examining the stability of nonlinear sampled-data control systems in the frequency domain.

It was pointed out in Chapter II that the stability of the nonlinear sampled-data control system could be obtained from a frequency phase plot of the open-loop transfer function, $N(\alpha) HG^*(s)$. The work in this thesis was limited to the problem of finding a way to obtain a plot of $N(\alpha) HG^*(s)$ on a Nyquist diagram.

A suitable procedure of evaluation was evolved and follows:

1. Calculate the frequency response of the linear portion of the system. This is accomplished by

using the series

$$HG^*(s) = \frac{1}{T} \sum_{n=-\infty}^{\infty} HG(s + jn\omega_s). \quad (41)$$

Each term of the right-hand side of the series can be represented by a vector. The vectorial sum of these will yield $HG^*(s)$. Fortunately, this sum usually can be represented by two or three terms of this series.

2. Make a Fourier series analysis of the output waveform from the nonlinear element when a sinusoidal is applied to the input.
3. Replace the nonlinear element with a first approximation for the nonlinear element by using the describing-function. The describing-function is the ratio of the fundamental to the sinusoidal input to the element.
4. Multiply the frequency response obtained (in 1 above) by the describing-function. This result will be the frequency phase plot for the nonlinear sampled-data control system, when all higher-ordered harmonics from the nonlinear element are neglected.

The result, which is obtained from 4 above, is the frequency phase plot for a nonlinear sampled-data control system. The accuracy of this procedure is limited only to the degree that the higher-ordered harmonics, which are

present at the output of the nonlinear element, are neglected. If the magnitude of each harmonic is very small when compared to the fundamental, the result obtained (on the preceding page) will be very accurate; however, if the harmonics are not small when compared to the fundamental, the result will be poor.

The additional steps which should be taken to account for higher order harmonics and increase the accuracy of the calculations are:

5. Calculate the percentage harmonic relative to the fundamental.
6. Multiply this percentage by the linear frequency response of the system at the frequency of the harmonic.
7. Add this result, vectorially, to the result obtained in 4 (on preceding page).
8. Repeat step 6 for each of the harmonics that need considering (this will become apparent in the calculation process), and add each of these to 7 above.

It was found that the method as proposed for obtaining a frequency phase plot of a nonlinear sampled-data control system is very accurate. This accuracy was verified in the experimental study. The results of the analytical and experimental study can be seen in Figures 23 and 24. It also appears that the control engineer can use this method to examine the stability of a nonlinear

sampled-data control system by following the steps outlined in this thesis and utilizing techniques with which he is familiar.

The nonlinear element of the saturation-type increased the relative stability of the system.

Although this study covered, both analytically and experimentally, the nonlinearity of saturation in detail, it is felt that additional work should be done for other types of nonlinearities. The nonlinear element of backlash or hysteresis should be of particular interest because it is a very common occurrence in nature, and because the phase shift within the nonlinear element varies as the frequency to the element is varied.

Another area for additional study would be the case where several nonlinearities are combined into one element, such as saturation and dead zone, saturation and hysteresis, dead zone and hysteresis, etc. Furthermore, a study of systems which contain more than a single sampler would be of particular interest since these systems occur quite often in practice.

BIBLIOGRAPHY

1. Mullin, F. J. "Stability of Saturating Sampled-Data Systems," American Institute of Electrical Engineers - Part I Communications and Electronics, July, 1959, p. 270.
2. Tou and Kinnen. "Analysis of Nonlinear Sampled-Data Control Systems," American Institute of Electrical Engineers Transactions - Part II Application and Industry, January, 1960, pp. 386-394.
3. Aseltine, J. A., and R. A. Nesbit. "The Incremental Phase Plane for Nonlinear Sampled-Data Systems," Transactions of Institute of Radio Engineers on Automatic Control, August, 1960, pp. 159-165.
4. Tou, J. T. Digital and Sampled-Data Control Systems. New York: McGraw-Hill Book Co., Inc., 1959.
5. Nyquist, H. "Regeneration Theory," Bell System Technical Journal, 11 (1932), pp. 126-47.
6. Thaler, G. J., and R. G. Brown. Servomechanism Analysis. New York: McGraw-Hill Book Co., Inc., 1953, pp. 159-162.
7. Raggazzini, J. R., and G. F. Franklin. Sampled-Data Control Systems. New York: McGraw-Hill Book Co., Inc., 1958, p. 131.
8. Truxal, J. G. Automatic Feedback Control System Synthesis. New York: McGraw-Hill Book Co., Inc., 1959, p. 134.
9. Johnson, C. L. Analog Computer Techniques. New York: McGraw-Hill Book Company, Inc., 1956.

VITA

William Stahley

Candidate for the Degree of
Doctor of Philosophy

Thesis: STABILITY STUDY OF A NONLINEAR SAMPLED-DATA
CONTROL SYSTEM

Major Field: Electrical Engineering

Biographical:

Personal Data: Born near Stuttgart, Arkansas,
September 30, 1928, the son of Jess P. and
Margaret E. Stahley.

Education: Attended grade school near Stuttgart,
Arkansas and was graduated from Stuttgart High
School, Stuttgart, Arkansas in 1945; received
the Bachelor of Science degree in Electrical
Engineering in August, 1957, and received Master
of Science degree in Electrical Engineering in
May, 1959 from Oklahoma State University; com-
pleted requirements for the Doctor of Philosophy
degree in May, 1964.

Professional Experience: Served in the United States
Air Force from 1950 to 1954; employed as a proj-
ect engineer from 1957 to 1958 at Sandia
Corporation; taught part-time for the School of
Electrical Engineering while working toward the
Master of Science and Doctor of Philosophy de-
grees at Oklahoma State University; employed as
a Senior Research Engineer at Autometrics from
1961 to present.